Energy Conversion and Management 161 (2018) 266–283

Contents lists available at ScienceDirect

Energy Conversion and Management

journal homepage: www.elsevier.com/locate/enconman

Smart wind speed forecasting using EWT decomposition, GWO evolutionary optimization, RELM learning and IEWT reconstruction

Hui Liu*, Haiping Wu, Yanfei Li

Institute of Artificial Intelligence and Robotics (IAIR), Key Laboratory of Traffic Safety on Track of Ministry of Education, School of Traffic and Transportation Engineering, Central South University, Changsha 410075, Hunan, China

ARTICLE INFO

Keywords:
Wind speed forecasting
Hybrid model
Empirical wavelet transform
Regularized extreme learning machine
Grey wolf optimizer
Inverse empirical wavelet transform

ABSTRACT

The high-precision forecasting of wind speed is of great significance for the wind power exploitation. In this study, a new hybrid model is presented, which combines the EWT (*Empirical Wavelet Transform)* decomposition, the GWO (*Grey Wolf Optimizer*) algorithm, the RELM (*Regularized Extreme Learning Machine*) network and the IEWT (*Inverse Empirical Wavelet Transform*) reconstruction. In the proposed structure, to realize the high-precision wind speed prediction, the hybrid modeling strategy has been used as: the EWT is adopted to decompose the raw series into several wind speed subseries adaptively; the RELM network optimized by GWO is employed to forecast each subseries; At the end of the forecasting computation, the IEWT is utilized to reconstruct the forecasted results to avoid the unexpected forecasting values. To evaluate the performance of the proposed model, eleven models are implemented in four forecasting experimental cases. The experimental results of four metrics show that: (1) the IEWT is effective in improving the accuracy and stability of the prediction; (2) the GWO improves the forecasting performance of the proposed hybrid EWT-RELM-IEWT structure significantly; (3) the performance of the RELM network is better than that of the SVM (*Support Vector Machine*) in the proposed hybrid EWT-GWO-IEWT structure; (4) in the involved forecasting models, the proposed hybrid model has the best multiple step prediction performance.

1. Introduction

In recent years, the growing environmental awareness has prompted the utilization and application of renewable energy widely. As an important source of renewable energy, the wind power is developing fast [1]. Owing to the intermittent and uncertain characteristics of the wind speed, it becomes difficult to balance the input and output power in the electricity system [2]. Making an accurate prediction of the wind speed in the wind farm is of great significance to overcome the above mentioned challenge [3]. Through a review of the previous literatures, many attempts have been made to predict the short-term wind speed [4]. The proposed works can be divided into physical methods [5], conventional statistical methods [6], intelligent approaches [7], and hybrid models [8]. Since the hybrid models have the ability of taking advantage of different methodologies and providing satisfactory forecasting performance, the hybrid models have received increasing attention [9]. In the hybrid model, there is a popular wind speed processing and forecasting structure. The signal decomposing methods are utilized to decrease the jumping performance of the raw wind speed data [10]. Some artificial intelligence approaches are used to realize the real forecasting computation [11]. In addition, different forms of error correction algorithms are involved in the hybrid structure to further improve the final forecasting performance by removing the unexpected wind speed forecasting values [12].

In the wind speed decomposing fields, there are many interesting works. For instance, Li et al. [13] built a hybrid model based on the BPNN (*Back Propagation Neural Network*), the ENN (*Elman Neural Network*) and the ARIMA (*Auto Regressive Integrated Moving Average*), in which the EMD (*Empirical Mode Decomposition*) was utilized to improve the prediction performance by disintegrating the wind speed series into the sum of many time series. In their study, the main features was extracted from the original series by the EMD. Their detailed case studies evaluated that the accuracy were greatly improved when using the wind speed series processed by the EMD. Wang et al. [14] proposed a hybrid prediction method based on the EEMD (*Ensemble Empirical Mode Decomposition*), the GA (*Genetic Algorithm*), and the BPNN. In their paper, the original time series were decomposed into a number of more stationary subsequences by the EEMD. Sun et al. [15] built a short-term wind speed forecasting model by combining the FEEMD (*Fast Ensemble Empirical Mode Decomposition*), the sample entropy algorithm, the phase

* Corresponding author.
E-mail address: csuliuhui@csu.edu.cn (H. Liu).

https://doi.org/10.1016/j.enconman.2018.02.006
Received 19 January 2018; Accepted 3 February 2018
Available online 09 February 2018
0196-8904/

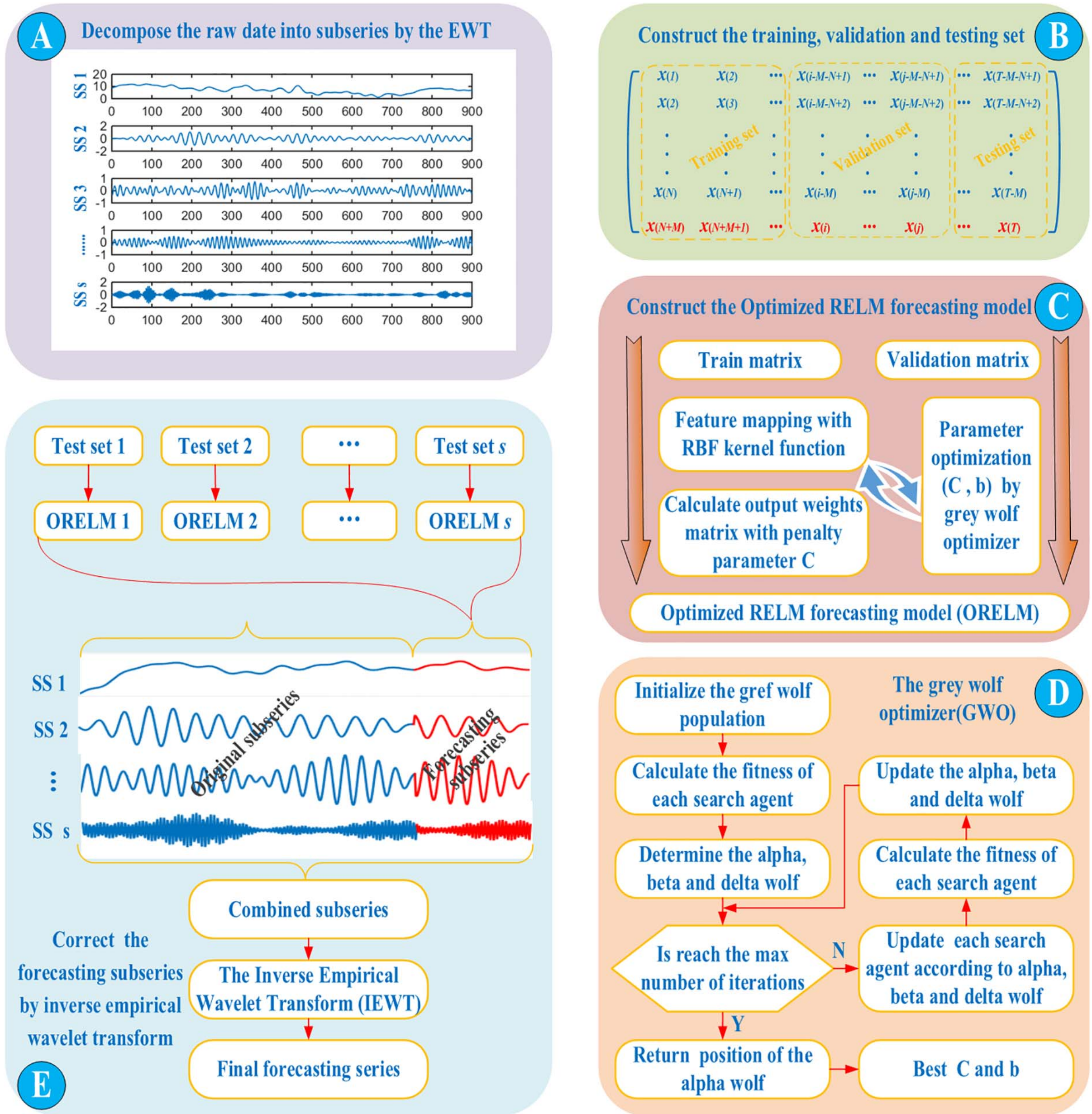

Fig. 1. The whole process of the EWT-GWO-RELM-IEWT model.

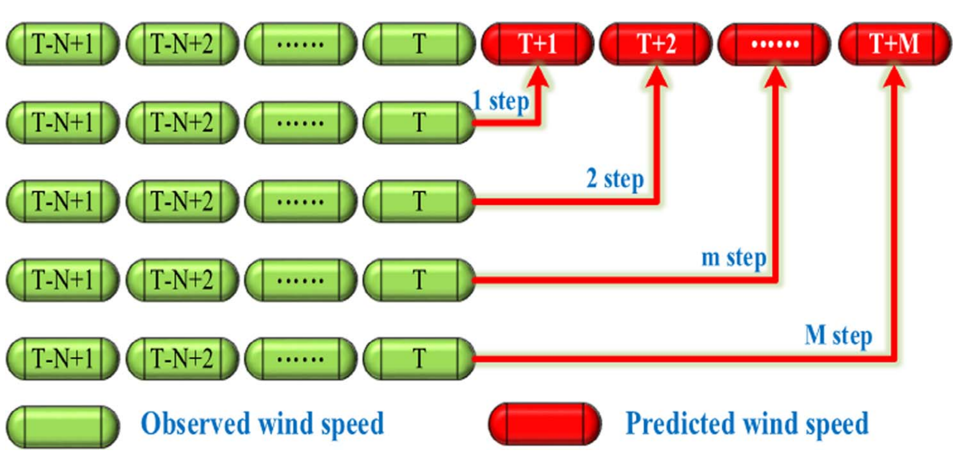

Fig. 2. The structure of multistep ahead forecasting.

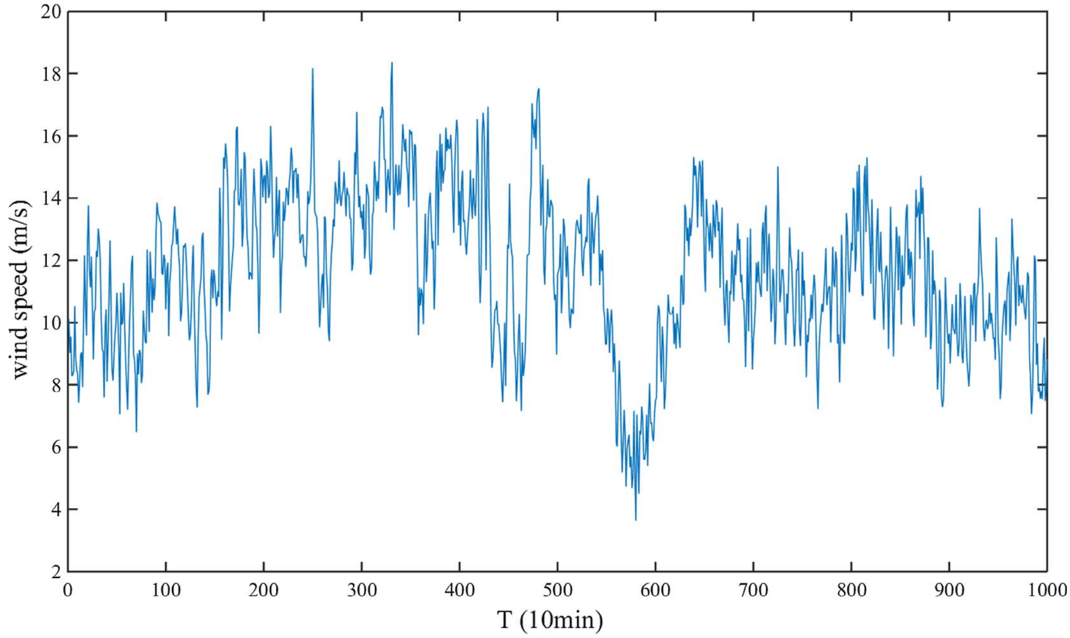

Fig. 3. Original wind speed time series #1.

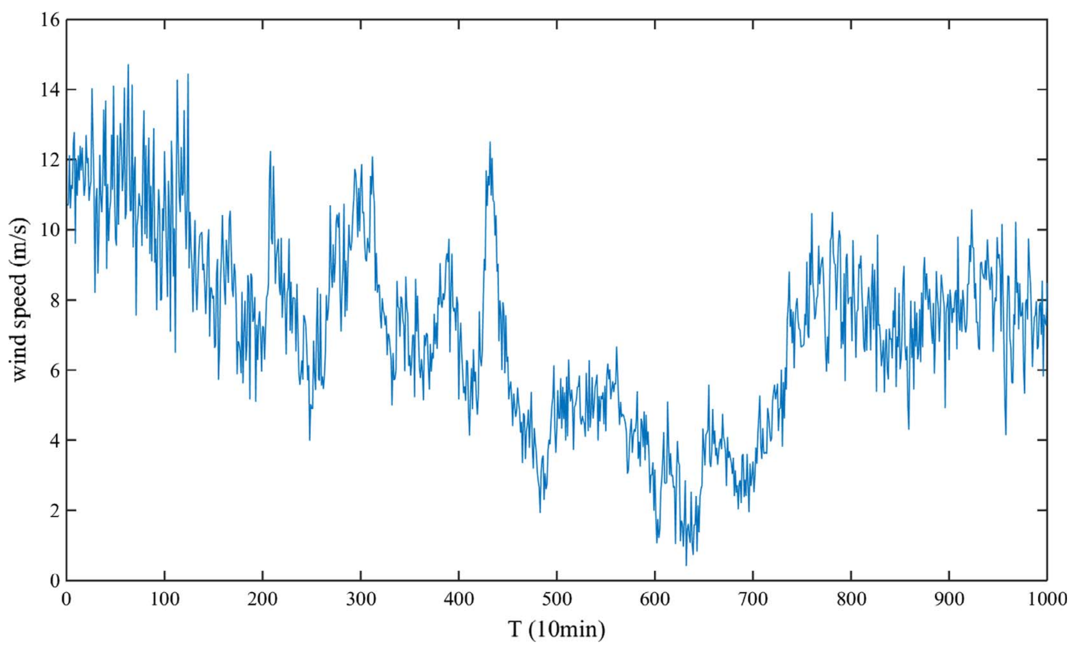

Fig. 4. Original wind speed time series #2.

space reconstruction theory and the BPNN. The FEEMD decomposition was executed to process the raw wind speed signals. Zhang et al. [16] presented a wind speed forecasting method based on the CEEMDAN (*Complete Ensemble Empirical Mode Decomposition Adaptive Noise*), the CLSFPA (*flower pollination algorithm with chaotic local search*), five neural networks and the NNCT (*no negative constraint theory*). The proposed conclusions showed that the proposed combined model had the best performance by comparing it with the single neural network models and the benchmark ARIMA model. Yu et al. [17] firstly predicted the wind speed signals by combining the WT (*Wavelet Transform*), the SSA (*Singular Spectrum Analysis*) and the ENN model. The traditional WT computation was employed in their work. The effectiveness of the proposed process was validated by several experiments. Liu et al. [18] carried out the wind speed forecasting by combining the WPD (*Wavelet Packet Decomposition*) and the ELM (*Extreme Learning Machine*). The combination model got a satisfactory result in the wind speed accurate predictions. It was proved that the WPD had better wind speed decomposing performance than the WT.

Every signal decomposing algorithm has two sides. For example, the WT and the WPD lack the ability to extract the deep information of the signals as much as possible, while the EMD, EEMD, FEEMD and CEEMDAN have insufficient mathematical definition. The EWT is a novel signal process tool, which can overcome the drawbacks of the aforementioned decomposition methodologies [19]. In Ref. [20], the EWT was employed to extract the meaningful information from the wind speed series by discarding the residual signal from the decomposed modes. Hu et al. [21] established a hybrid model based on the EWT and the GPR-*t* (*Gaussian Process Regression with the student-t*

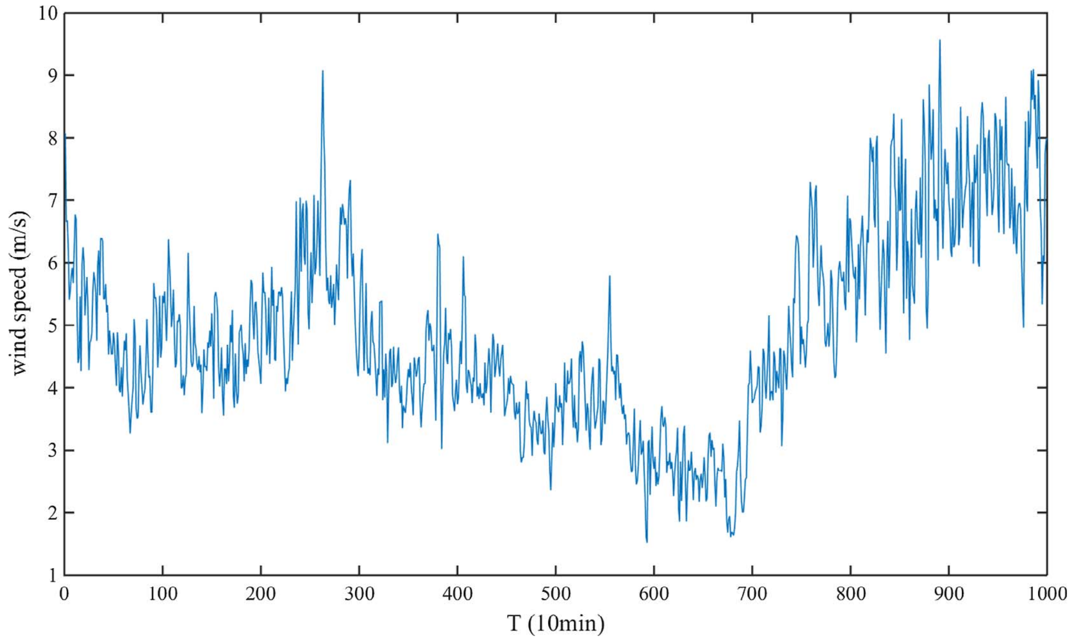

Fig. 5. Original wind speed time series #3.

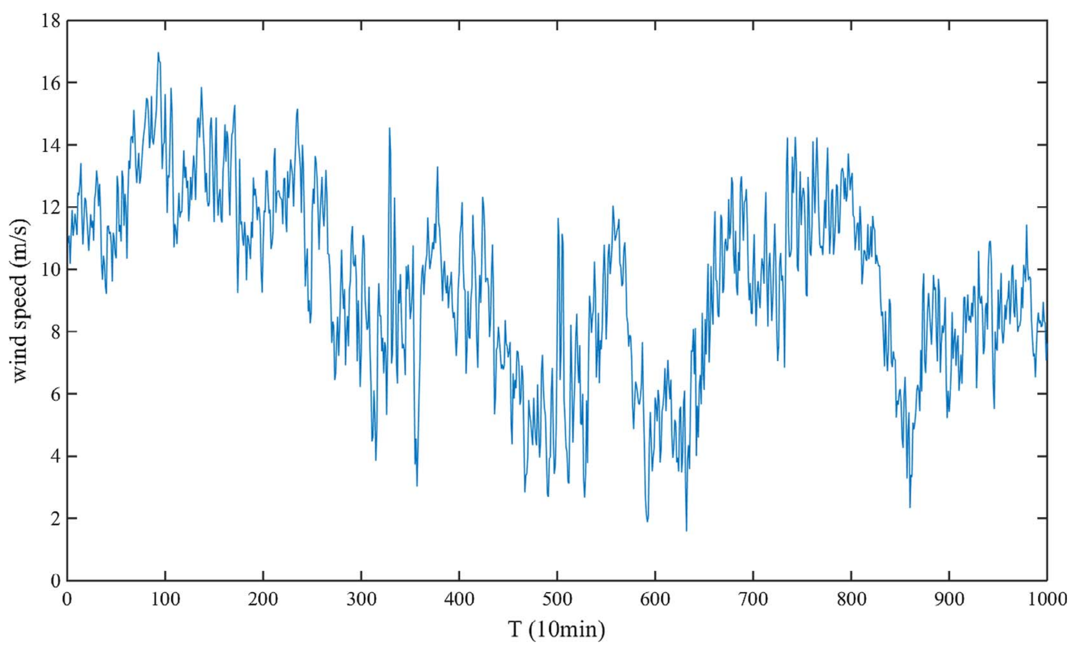

Fig. 6. Original wind speed time series #4.

observation) model. In the proposed hybrid model, the EWT was untiled to decompose the original signals into several modes and the noisy residuals were filtered out at the same time. The numerical experimental results demonstrated that the proposed model could provide satisfactory interval forecasting compared to the contrast models. Liu et al. [22] proposed a model that combine the EWT with two kinds of RNN (*Recurrent Neural Network*) and got competitive performance in the high-precision wind speed prediction.

With the development of the artificial intelligent techniques, the artificial intelligence models have been widely used in the wind speed forecasting [23]. Jiang et al. [24] studied a structure consisting of the grey correlation analysis and the *ν*-SVM (*ν-Support Vector Machine*) optimized by the cuckoo algorithm. Their experimental results indicated that the difference between the *ν*-SVM and the ε-SVM (*ε-Support Vector Machine*) was nonsignificant in the proposed wind speed forecasting structure. Ren et al. [25] proposed a succinct wind speed forecasting model based on the SVR (*Support Vector Regression*) and the EMD, in which several intrinsic mode functions were used to train the SVR. Qu et al. [26] provided an ensemble model based on the BPNN, the RBFNN (*Radial Basis Function Neural Network*), the GRNN (*Generalized Regression Neural Network*) and the WNN (*Wavelet Neural Network*). In the study, the suitable coefficients of these models were determined by the MOBSFPA (*Multi-Objective Bat-search Flower-Pollination Algorithm*). Niu et al. [27] established a multistep ahead wind speed prediction model through optimizing the ANN (artificial neural network) by a modified bat algorithm. Liu et al. [28] put forward a hybrid framework, which was comprised of the WPD, the EEMDAN and the ANN. the experimental results showed that the hybrid framework had better three-step prediction performance than individual ANN models.

In the field of artificial intelligence, the extreme learning machine

Table 1
The error estimated results of different models for the wind speed series #1.

Forecasting models	Step	MAPE (%)	MAE (m/s)	RMSE (m/s)	SDE (m/s)
RELM	1	8.9127	0.8790	1.1410	1.1353
	2	12.5070	1.2178	1.4698	1.4487
	3	12.9922	1.2409	1.5332	1.4874
	4	13.0318	1.2219	1.5588	1.4730
	5	13.1898	1.2291	1.5243	1.3845
	6	13.8346	1.2946	1.5620	1.3887
	7	14.2242	1.3337	1.6176	1.4333
GWO-RELM	1	8.8490	0.8657	1.1034	1.0916
	2	12.2216	1.1569	1.3990	1.3279
	3	12.8467	1.2217	1.4885	1.4285
	4	12.8301	1.2032	1.4820	1.3862
	5	13.0118	1.2211	1.4881	1.3824
	6	13.3826	1.2589	1.5201	1.3984
	7	14.1144	1.3274	1.5868	1.4400
EWT-RELM -IEWT	1	1.2934	0.1230	0.1584	0.1505
	2	1.7709	0.1683	0.2125	0.1967
	3	2.2268	0.2126	0.2644	0.2378
	4	2.7612	0.2632	0.3317	0.2931
	5	3.4294	0.3258	0.4081	0.3559
	6	4.1556	0.3940	0.4866	0.4192
	7	4.8775	0.4621	0.5615	0.4757
EWT-GWO -RELM	1	0.6798	0.0677	0.0886	0.0885
	2	0.7833	0.0777	0.1015	0.1014
	3	0.9317	0.0926	0.1179	0.1174
	4	1.2004	0.1198	0.1500	0.1484
	5	1.4386	0.1431	0.1841	0.1818
	6	1.7654	0.1736	0.2211	0.2119
	7	2.0841	0.2038	0.2507	0.2381
EWT-GWO -RELM-IEWT	1	0.2123	0.0212	0.0268	0.0261
	2	0.3752	0.0372	0.0476	0.0468
	3	0.4912	0.0492	0.0620	0.0599
	4	0.7385	0.0740	0.0930	0.0899
	5	1.0296	0.1025	0.1273	0.1160
	6	1.4135	0.1396	0.1788	0.1656
	7	1.7755	0.1756	0.2129	0.1973
EWT-GWO -SVM-IEWT	1	2.0191	0.1909	0.2527	0.2433
	2	2.4056	0.2299	0.2813	0.2467
	3	2.8305	0.2717	0.3295	0.2617
	4	3.4645	0.3337	0.4206	0.3144
	5	3.8723	0.3720	0.4666	0.3321
	6	4.1023	0.3929	0.4890	0.3513
	7	4.2567	0.4054	0.5027	0.3867
VMD-GWO -RELM	1	6.9156	0.6812	0.8634	0.8559
	2	11.6212	1.1182	1.3492	1.3197
	3	12.3819	1.1699	1.4276	1.3660
	4	12.6611	1.1863	1.4580	1.3673
	5	12.5674	1.1818	1.4474	1.3659
	6	12.8959	1.2140	1.4814	1.3828
	7	14.0077	1.3016	1.5595	1.3892
EMD-GWO -RELM	1	6.6224	0.6467	0.7883	0.7827
	2	8.6006	0.8224	1.0134	1.0041
	3	11.2245	1.0506	1.3427	1.3145
	4	11.2501	1.0510	1.3473	1.3150
	5	11.2973	1.0565	1.3499	1.3199
	6	11.4557	1.0711	1.3619	1.3302
	7	12.5424	1.1804	1.4818	1.4611
EEMDAN -GWO-RELM	1	5.6512	0.5560	0.6915	0.6904
	2	7.4353	0.7282	0.9118	0.9097
	3	8.9269	0.8719	1.0997	1.0992
	4	8.3246	0.8100	1.0303	1.0288
	5	7.6991	0.7506	0.9287	0.9280
	6	10.8057	1.0467	1.2853	1.2833
	7	9.1156	0.8869	1.1321	1.1313
WT-GWO -RELM	1	2.0198	0.1969	0.2419	0.2417
	2	4.1131	0.4090	0.5074	0.5071
	3	4.1029	0.4099	0.5196	0.5191
	4	4.8625	0.4814	0.6059	0.6040
	5	7.6355	0.7478	0.9203	0.9143
	6	7.5791	0.7478	0.9232	0.9188
	7	9.1645	0.8881	1.0872	1.0847
WPD-GWO -RELM	1	0.3631	0.0361	0.0447	0.0437
	2	0.5994	0.0603	0.0750	0.0740
	3	1.0202	0.1012	0.1299	0.1280
	4	1.3766	0.1369	0.1814	0.1779
	5	1.9075	0.1871	0.2372	0.2319
	6	2.5258	0.2472	0.3020	0.2922
	7	3.2817	0.3206	0.3822	0.3649

was originally put forward for training the SLFNs (*Single-hidden Layer Feed Forward Neural Networks*) [29]. With faster learning speed and impressive generalization performance, it had also been used in the field of wind speed forecasting [30]. Zhang et al. [31] proposed a combined structure for the short-term wind speed forecasting, in which the wind speed signal was decomposed into a few modes by the OVMD (*Optimized Variation Mode Decomposition*). Each decomposed mode was predicted by the ELM, whose parameters were optimized by the HBSA (*Hybrid Backtracking Search Algorithm*). Sun et al. [32] carried out the short-term wind speed forecasting by combining the RELM (*Regularized Extreme Learning Machine*) and the FEEMD. Zheng et al. [33] studied a structure named the CQR-ORELM (*Composite Quantile Regression Outlier-robust Extreme Learning Machine*) for the short-term wind speed forecasting. In the structure, a hybrid optimizer was proposed by combining the gravitational search algorithm and the particle swarm optimization.

To improve the performance of the forecasting models further, some error processing techniques were put forward. Wang et al. [34] built a GARCH (*Generalized Autoregressive Conditional Heteroscedasticity*) model to simulate the residual series and compensate the main model. In Ref. [35], an outlier correction method was proposed, which corrected the outlier via an average mechanism in the time domain. Liu et al. [36] proposed a novel hybrid model where the WT was utilized to process the forecasted series to get the final forecasting series. It was proved that the post processing was effective to further improve the wind speed forecasting performance.

Inspired by the above-mentioned hybrid structure, in the study a novel model is proposed using the EWT decomposition, the GWO algorithm, the RELM neural network and the IEWT reconstruction. The contribution of the proposed hybrid forecasting model can be summarized as follows: (a) The EWT, which generates wavelet adaptively according to the spectral distribution of the wind speed series, is adopted to decompose the raw series into several subseries. Compared to other signal decomposing algorithms (*e.g., the WT, the WPD, the EMD, the CEEMDAN etc.*), it is proved that the adopted EWT algorithm has the integral performance of the EMD and the WT. The real performance of the EWT decomposition in the wind speed forecasting fields has not been investigated before; (b) The RELM network which optimized by GWO is used to forecast each decomposed wind speed subseries obtained by the EWT. It is interesting to investigate the promoting possibility of the original RELM network by the GWO algorithm. The combination of the RELM network and the GWO algorithm in the wind speed forecasting has also been not published before. Especially, it is really interesting that the performance of the hybrid GWO-RELM model will be studied in the EWT based signal decomposing framework; and (c) it can be predicted that the EWT algorithm could have good performance in the wind speed decomposing computation. However, in the study, the EWT algorithm will not be only used to complete the original wind speed decomposition, but also to do the signal reconstruction for the final forecasted wind speed values. The purpose of the IEWT based reconstruction is to correct the unexpected forecasting wind speed values generated by the built hybrid GWO-RELM predictor.

Table 2
The error estimated results of different models for the wind speed series #2.

Forecasting models	step	MAPE (%)	MAE (m/s)	RMSE (m/s)	SDE (m/s)
RELM	1	13.0638	0.9714	1.2461	1.2460
	2	14.8143	1.0891	1.3938	1.3937
	3	15.7723	1.1668	1.5109	1.5090
	4	16.4687	1.2284	1.5456	1.5422
	5	15.4419	1.1624	1.5172	1.5100
	6	15.2518	1.1465	1.5011	1.4891
	7	15.1095	1.1400	1.4463	1.4251
GWO-RELM	1	12.6113	0.9273	1.2003	1.1996
	2	14.3508	1.0450	1.3585	1.3582
	3	15.3144	1.1223	1.4537	1.4536
	4	15.9019	1.1674	1.4791	1.4780
	5	15.3511	1.1319	1.4492	1.4480
	6	15.0488	1.1050	1.4385	1.4377
	7	14.7055	1.0712	1.4054	1.4052
EWT-RELM -IEWT	1	2.5220	0.1902	0.2409	0.2398
	2	2.8007	0.2129	0.2622	0.2582
	3	3.0566	0.2349	0.2862	0.2765
	4	3.4912	0.2706	0.3276	0.3094
	5	3.9997	0.3111	0.3776	0.3481
	6	4.5281	0.3536	0.4274	0.3848
	7	5.0846	0.3987	0.4845	0.4252
EWT-GWO -RELM	1	1.0581	0.0808	0.0992	0.0992
	2	1.1269	0.0865	0.1072	0.1072
	3	1.1931	0.0921	0.1147	0.1147
	4	1.3741	0.1062	0.1328	0.1327
	5	1.6825	0.1311	0.1641	0.1637
	6	1.8888	0.1460	0.1807	0.1802
	7	2.1050	0.1639	0.2039	0.2029
EWT-GWO -RELM-IEWT	1	0.4812	0.0365	0.0436	0.0436
	2	0.5965	0.0455	0.0552	0.0552
	3	0.7195	0.0555	0.0666	0.0665
	4	0.9114	0.0707	0.0849	0.0847
	5	1.1675	0.0906	0.1082	0.1079
	6	1.4157	0.1101	0.1328	0.1324
	7	1.6426	0.1283	0.1562	0.1556
EWT-GWO -SVM-IEWT	1	2.8708	0.2200	0.2756	0.2747
	2	2.7775	0.2114	0.2610	0.2608
	3	2.9464	0.2257	0.2835	0.2717
	4	3.5591	0.2801	0.3445	0.3080
	5	3.6591	0.2772	0.3370	0.3370
	6	4.2390	0.3221	0.3820	0.3818
	7	4.7549	0.3802	0.4676	0.3725
VMD-GWO -RELM	1	7.5949	0.5639	0.7284	0.7278
	2	13.9122	1.0139	1.3072	1.3064
	3	14.9255	1.0902	1.4192	1.4188
	4	15.7549	1.1570	1.4760	1.4750
	5	15.2862	1.1271	1.4404	1.4392
	6	15.1177	1.1125	1.4324	1.4311
	7	14.9091	1.0855	1.4228	1.4215
EMD-GWO -RELM	1	9.8010	0.7361	0.9281	0.9008
	2	9.8341	0.7382	0.9329	0.9049
	3	10.3523	0.7959	0.9926	0.9557
	4	10.9197	0.8287	1.0598	1.0325
	5	10.9589	0.8289	1.0600	1.0386
	6	11.4901	0.8640	1.0991	1.0803
	7	11.5917	0.8754	1.1102	1.0863
EEMDAN -GWO-RELM	1	7.3416	0.5503	0.6770	0.6708
	2	8.8009	0.6490	0.8438	0.8411
	3	9.1426	0.6820	0.8819	0.8756
	4	10.4012	0.7776	0.9987	0.9880
	5	11.3609	0.8229	1.0815	1.0806
	6	10.5775	0.7957	1.0122	1.0015
	7	9.9612	0.7335	0.9569	0.9564
WT-GWO -RELM	1	1.7866	0.1306	0.1697	0.1697
	2	6.2862	0.4773	0.6255	0.6255
	3	6.4654	0.4862	0.6428	0.6423
	4	7.7113	0.5733	0.7417	0.7415
	5	7.4591	0.5590	0.7209	0.7209
	6	7.6156	0.5677	0.7300	0.7300
	7	10.5020	0.7821	0.9837	0.9831

Table 2 (*continued*)

Forecasting models	step	MAPE (%)	MAE (m/s)	RMSE (m/s)	SDE (m/s)
WPD-GWO -RELM	1	0.4538	0.0353	0.0455	0.0454
	2	4.2040	0.3201	0.3963	0.3962
	3	2.1822	0.1627	0.2173	0.2171
	4	1.3248	0.1011	0.1228	0.1228
	5	2.2952	0.1748	0.2308	0.2305
	6	4.7317	0.3569	0.4364	0.4361
	7	5.2129	0.3899	0.4678	0.4674

2. The hybrid EWT-GWO-RELM-IEWT model

2.1. The whole process of the proposed model

The architecture of the hybrid EWT-GWO-RELM-IEWT model is depicted as given in Fig. 1.. The detailed descriptions are further explained as follows:

(1) The EWT algorithm is utilized to decompose the original wind speed data into a series of subseries. *The details of the EWT algorithm are given in Section 2.2*.

(2) The original wind speed data are constructed into the training sets, the validation sets and the testing sets. The input and output matrixes in each data set are constructed according to the data processing structure as proposed in Fig. 2..

(3) The RELM model is built to forecast the decomposed wind speed data and the GWO algorithm is adopted to optimize the parameters of the built RELM models. *The details of the RELM and GWO are described in Section 2.3 and Section 2.4*.

(4) The forecasting results of each subseries are combined with the corresponding original subseries. The Fourier spectrum segments of the original subseries are acquired as the estimation value of the combined series. The IEWT algorithm is used to reconstruct the combined wind speed series.

(5) The horizon of 1-step to 7-step ahead predictions are investigated in this study. To evaluate the prediction performance of the proposed hybrid EWT-GWO -RELM-IEWT model, ten different forecasting models are included in the performance comparison. They consist of the single RELM model, the hybrid GWO-RELM model, the hybrid EWT-RELM-IEWT model, the hybrid EWT-GWO-RELM model, the hybrid EWT-GWO-SVM-IEWT model, the hybrid VMD-GWO-RELM model, the hybrid EMD-GWO-RELM model, the hybrid EEMDAN-GWO-RELM model, the hybrid WT-GWO-RELM model and the hybrid WPD-GWO-RELM model. *The details of the performance evaluation indexes are illustrated in Section 2.5, and the analysis is illustrated in Section 3 and 4*.

2.2. Empirical wavelet transform

The EWT builds a set of band pass filters whose supports depend on the information of the spectrum of the analyzed signal [37]. As shown in Ref. [37], the EWT can be carried out as follows: firstly, we segment the Fourier support $[0,\pi]$ into N contiguous segments, in which the $\omega_n$is the separatrix. Each segment is denoted as $\Lambda_n = [\omega_{n-1},\omega_{n-1}]$. The empirical scaling function and the empirical wavelets are further explained in (1) and (2), respectively:

$$\hat{\phi}_n(\omega) = \begin{cases} 1 & if|\omega| \leqslant (1-\gamma)\omega_n \\ \cos\left[\frac{\pi}{2}\beta\left(\frac{1}{2\gamma\omega_n}(|\omega|-(1-\gamma)\omega_n)\right)\right] & if\,(1-\gamma)\omega_n \leqslant |\omega| \leqslant (1+\gamma)\omega_n \\ 0 & otherwise \end{cases} \quad (1)$$

Table 3
The error estimated results of different models for the wind speed series #3.

Forecasting models	Step	MAPE (%)	MAE (m/s)	RMSE (m/s)	SDE (m/s)
RELM	1	9.7515	0.7255	0.9323	0.8770
	2	11.7886	0.8779	1.0881	1.0041
	3	12.0896	0.9067	1.1184	0.9935
	4	12.5202	0.9433	1.1566	0.9868
	5	12.4498	0.9485	1.1955	0.9795
	6	13.3265	1.0162	1.2685	1.0257
	7	13.5975	1.0377	1.2969	1.0388
GWO-RELM	1	8.7455	0.6450	0.8497	0.8202
	2	11.4142	0.8383	1.0027	0.9443
	3	11.4687	0.8494	1.0360	0.9459
	4	12.3473	0.9172	1.1073	0.9867
	5	11.8891	0.8980	1.1081	0.9252
	6	12.2698	0.9331	1.1551	0.9395
	7	12.5972	0.9610	1.1986	0.9642
EWT-RELM -IEWT	1	3.4068	0.2579	0.3197	0.2519
	2	3.8105	0.2888	0.3569	0.2662
	3	4.2921	0.3259	0.4055	0.2931
	4	4.8886	0.3704	0.4595	0.3259
	5	5.5522	0.4207	0.5203	0.3563
	6	6.2871	0.4761	0.5866	0.3929
	7	7.0668	0.5355	0.6566	0.4297
EWT-GWO -RELM	1	0.8856	0.0639	0.0824	0.0760
	2	1.0675	0.0778	0.1000	0.0891
	3	1.3571	0.0992	0.1277	0.1110
	4	1.6395	0.1193	0.1509	0.1238
	5	2.2951	0.1673	0.2106	0.1769
	6	2.8038	0.2067	0.2688	0.2254
	7	3.2256	0.2366	0.3045	0.2424
EWT-GWO -RELM-IEWT	1	0.5839	0.0433	0.0556	0.0477
	2	0.7712	0.0579	0.0760	0.0632
	3	1.2209	0.0913	0.1198	0.1043
	4	1.3600	0.1025	0.1338	0.1076
	5	1.7434	0.1309	0.1710	0.1390
	6	2.1495	0.1610	0.2090	0.1587
	7	2.6913	0.2020	0.2584	0.1873
EWT-GWO -SVM-IEWT	1	3.3233	0.2521	0.3045	0.1796
	2	3.2307	0.2455	0.2964	0.1791
	3	3.1586	0.2396	0.2871	0.1746
	4	3.2605	0.2453	0.2991	0.1964
	5	3.6772	0.2747	0.3373	0.2276
	6	3.9741	0.2965	0.3671	0.2501
	7	4.2469	0.3182	0.3939	0.2606
VMD-GWO -RELM	1	5.7615	0.4217	0.5459	0.5320
	2	11.2920	0.8274	1.0061	0.9670
	3	12.2774	0.9056	1.1111	1.0419
	4	12.2189	0.9059	1.0984	0.9900
	5	11.8286	0.8893	1.0865	0.9280
	6	12.0314	0.9132	1.1259	0.9283
	7	12.3400	0.9410	1.1727	0.9519
EMD-GWO -RELM	1	6.5932	0.4770	0.5579	0.5478
	2	7.4438	0.5354	0.6524	0.6454
	3	7.6246	0.5483	0.6681	0.6601
	4	7.9858	0.5774	0.7119	0.6932
	5	8.8570	0.6475	0.8196	0.7993
	6	8.9723	0.6421	0.7770	0.7690
	7	9.5979	0.7012	0.8531	0.8252
EEMDAN -GWO-RELM	1	7.2750	0.5513	0.6747	0.4826
	2	8.2062	0.6154	0.7469	0.6252
	3	8.8343	0.6594	0.7969	0.6843
	4	8.6980	0.6462	0.7985	0.7222
	5	9.1907	0.6842	0.8190	0.7157
	6	9.2801	0.6882	0.8257	0.7384
	7	15.4721	1.1860	1.3914	0.8526
WT-GWO -RELM	1	1.6568	0.1193	0.1530	0.1485
	2	4.5383	0.3295	0.3963	0.3901
	3	5.8242	0.4211	0.5149	0.5119
	4	6.4731	0.4686	0.5499	0.5428
	5	8.9954	0.6490	0.7889	0.7734
	6	9.0703	0.6538	0.7925	0.7776
	7	7.7348	0.5683	0.6816	0.6347
WPD-GWO -RELM	1	1.2101	0.0880	0.1093	0.1048
	2	1.2509	0.0918	0.1162	0.1093
	3	1.7114	0.1258	0.1566	0.1394
	4	3.0560	0.2239	0.3089	0.2971
	5	3.0638	0.2285	0.3010	0.2707
	6	3.5750	0.2679	0.3410	0.2892
	7	4.8030	0.3542	0.4256	0.3695

$$\hat{\psi}_n(\omega) = \begin{cases} 1 & if\ (1+\gamma)\omega_n \leqslant |\omega| \leqslant (1-\gamma)\omega_{n+1} \\ \cos\left[\frac{\pi}{2}\beta\left(\frac{1}{2\gamma\omega_{n+1}}(|\omega|-(1-\gamma)\omega_{n+1})\right)\right] & if\ (1-\gamma)\omega_{n+1} \leqslant |\omega| \leqslant (1+\gamma)\omega_{n+1} \\ \sin\left[\frac{\pi}{2}\beta\left(\frac{1}{2\gamma\omega_{n}}(|\omega|-(1-\gamma)\omega_{n})\right)\right] & if\ (1-\gamma)\omega_n \leqslant |\omega| \leqslant (1+\gamma)\omega_n \\ 0 & otherwise \end{cases} \tag{2}$$

where $\gamma \in (0,1)$ is a ratio which controls the width of the transition phase. To ensure the set $\{\phi_1(t),\{\psi_n(t)\}_{n=1}^{N}\}$ is a tight frame of $L^2(R)$, the following equation is defined as:

$$\gamma < \min_n\left(\frac{\omega_{n+1}-\omega_n}{\omega_{n+1}+\omega_n}\right) \tag{3}$$

the function $\beta(x)$ is an arbitrary $C^k([0,1])$ function that meets the following criteria as:

$$\beta(x) = \begin{cases} 0 \text{ if } x \leqslant 0 \\ 1 \text{ if } x \geqslant 1 \end{cases} \text{and} \beta(x) + \beta(1-x) = 1\ \forall\ x \in [0,1] \tag{4}$$

As defined in Ref. [37], the approximation coefficients are computed by the inner product with the scaling function as:

$$w_f^{\varepsilon}(0,t) = \langle f,\phi_1\rangle = \int f(\tau)\overline{\phi_1(\tau-t)}d\tau = (\hat{f}(\omega)\overline{\hat{\phi}_1(\omega)})^{\vee} \tag{5}$$

And the detail coefficients are computed by the inner product with the empirical wavelets as:

$$w_f^{\varepsilon}(n,t) = \langle f,\psi_n\rangle = \int f(\tau)\overline{\psi_n(\tau-t)}d\tau = (\hat{f}(\omega)\overline{\hat{\psi}_n(\omega)})^{\vee} \tag{6}$$

As shown in Ref. [37], the original signal can be decomposed to several empirical modes which are defined as:

$$f_0(t) = w_f^{\varepsilon}(0,t)*\phi_1 \tag{7}$$

$$f_k(t) = w_f^{\varepsilon}(k,t)*\psi_k \tag{8}$$

And the reconstruction can be obtained by the following equation as:

$$f(t) = w_f^{\varepsilon}(0,t)*\phi_1(t) + \sum_{n=1}^{N} w_f^{\varepsilon}(n,t)*\psi_n(t) = \left(\hat{w}_f^{\varepsilon}(0,\omega)\hat{\phi}_1(\omega) + \sum_{n=1}^{N}\hat{w}_f^{\varepsilon}(n,\omega)\hat{\psi}_n(\omega)\right)^{\vee} \tag{9}$$

2.3. Regularized extreme learning machine

The ELM, which was proposed by Huang [38], is a novel structure for training the SLFNs. The output weights of the ELM are determined by the matrix operation other than the iterative tuning. As shown in Ref. [38], the primary mission of the classical ELM is to get a solution of the β that satisfies as:

Table 4
The error estimated results of different models for the wind speed series #4.

Forecasting models	Step	MAPE (%)	MAE (m/s)	RMSE (m/s)	SDE (m/s)
RELM	1	9.5018	0.7636	0.9581	0.9578
	2	11.4600	0.9205	1.1457	1.1453
	3	11.9479	0.9565	1.2416	1.2359
	4	13.2686	1.0483	1.2917	1.2905
	5	13.8164	1.1020	1.3728	1.3677
	6	13.9563	1.1179	1.3953	1.3933
	7	14.3654	1.1371	1.4148	1.4141
GWO-RELM	1	9.4734	0.7698	0.9512	0.9465
	2	10.9949	0.8820	1.1586	1.1566
	3	11.7272	0.9250	1.1960	1.1960
	4	12.8191	1.0256	1.3050	1.3002
	5	12.9611	1.0429	1.3149	1.3120
	6	12.7247	1.0316	1.2929	1.2893
	7	12.7895	1.0258	1.2684	1.2677
EWT-RELM -IEWT	1	1.3203	0.1093	0.1360	0.1321
	2	2.0268	0.1671	0.2043	0.1985
	3	2.8483	0.2335	0.2867	0.2790
	4	3.6908	0.3015	0.3752	0.3652
	5	4.5625	0.3746	0.4662	0.4533
	6	5.5941	0.4600	0.5679	0.5535
	7	6.6171	0.5405	0.6683	0.6553
EWT-GWO -RELM	1	0.9871	0.0812	0.1006	0.1005
	2	1.3187	0.1082	0.1351	0.1346
	3	1.7875	0.1462	0.1807	0.1803
	4	2.3038	0.1886	0.2445	0.2441
	5	2.7334	0.2232	0.2849	0.2845
	6	3.4599	0.2832	0.3529	0.3524
	7	4.0075	0.3247	0.4041	0.4028
EWT-GWO -RELM-IEWT	1	0.3327	0.0273	0.0341	0.0337
	2	0.6850	0.0559	0.0684	0.0676
	3	1.5011	0.1219	0.1514	0.1509
	4	1.8046	0.1460	0.1788	0.1783
	5	2.4260	0.1962	0.2423	0.2419
	6	2.9338	0.2355	0.2851	0.2843
	7	3.5657	0.2853	0.3448	0.3430
EWT-GWO -SVM-IEWT	1	1.5401	0.1263	0.1565	0.1555
	2	1.7800	0.1445	0.1801	0.1738
	3	1.9752	0.1612	0.2051	0.1859
	4	2.4942	0.2017	0.2495	0.2397
	5	3.2144	0.2590	0.3213	0.3084
	6	4.3023	0.3464	0.4339	0.4199
	7	5.3887	0.4317	0.5453	0.5374
VMD-GWO -RELM	1	6.3066	0.5121	0.6261	0.6237
	2	10.9982	0.8980	1.1425	1.1328
	3	11.6578	0.9402	1.2260	1.2153
	4	12.6912	1.0191	1.2949	1.2863
	5	13.0322	1.0519	1.3244	1.3176
	6	12.8321	1.0423	1.3083	1.3020
	7	12.9097	1.0390	1.2804	1.2781
EMD-GWO -RELM	1	6.2158	0.5177	0.6598	0.6376
	2	7.5618	0.6324	0.8629	0.8554
	3	7.5466	0.6274	0.8565	0.8536
	4	7.8466	0.6497	0.8714	0.8671
	5	9.3309	0.7610	0.9831	0.9810
	6	9.3864	0.7616	0.9861	0.9860
	7	9.5263	0.7750	1.0016	1.0002
EEMDAN -GWO-RELM	1	5.5948	0.4543	0.5749	0.5727
	2	6.4285	0.5287	0.6909	0.6858
	3	6.8878	0.5563	0.7071	0.7068
	4	7.2038	0.5914	0.7771	0.7740
	5	8.9780	0.7250	0.9283	0.9276
	6	7.8828	0.6488	0.8413	0.8315
	7	9.7774	0.7883	1.0062	1.0051
WT-GWO -RELM	1	4.7644	0.3906	0.4871	0.4871
	2	4.7861	0.3934	0.4941	0.4940
	3	4.7529	0.3906	0.5036	0.5034
	4	6.1500	0.5068	0.6590	0.6589
	5	5.1745	0.4258	0.5592	0.5584
	6	6.4703	0.5340	0.6924	0.6914
	7	6.6670	0.5516	0.7299	0.7276
WPD-GWO -RELM	1	0.3377	0.0271	0.0375	0.0375
	2	1.2710	0.0982	0.1599	0.1599
	3	2.7525	0.2163	0.2902	0.2901
	4	6.3745	0.5091	0.6134	0.6134
	5	5.6771	0.4587	0.5374	0.5370
	6	3.2037	0.2586	0.3281	0.3260
	7	6.3617	0.5157	0.6091	0.6078

$$\min_{\beta\in R^{L\times m}} \|H\beta - T\|^2 \tag{10}$$

where β is the output weight vector between the hidden layers of L nodes to the m output nodes, T is the $N\times m$ training data target matrix and H is the hidden layer output matrix as:

$$H = \begin{bmatrix} g(a_1,b_1,x_1) & \cdots & g(a_L,b_L,x_1) \\ \vdots & \vdots & \vdots \\ g(a_1,b_1,x_N) & \cdots & g(a_L,b_L,x_N) \end{bmatrix}_{N\times L} \tag{11}$$

where $\mathbf{x} = [x_1,x_2...x_N]^T$ is the input matrix, $g(a,b,x)$ is a nonlinear piecewise continuous function satisfying the ELM universal approximation capability theorems [39]. For instance, the Gaussian function is an alternative choice, where:

$$g(a,b,x) = e^{-b\|x-a\|^2} \tag{12}$$

In order to get better generalization performance, a regularized extreme learning machine is proposed in which both the training error and the norm of output weights are taken into consideration. As proposed in Ref. [39], the solution of the RELM can be described as an unconstrained optimization problem:

$$\min_{\beta\in R^{L\times m}} L_{RELM} = \frac{1}{2}\|\beta\|^2 + \frac{C}{2}\sum_{i=1}^{N} \|T - H\beta\|^2 \tag{13}$$

by setting $\frac{\partial L_{RELM}}{\partial \beta} = 0$, we have

$$L_{RELM} = \beta^* - CH^T(T - H\beta^*) = 0 \tag{14}$$

if H has more rows than columns, β^* can be computed as

$$\beta^* = \left(H^TH + \frac{I}{C}\right)^{-1} H^TT \tag{15}$$

where I is an identity matrix with a size of $L\times L$. If H has less rows than columns, it becomes an under-determined least squares problem. To solve the problem, another constraint is needed. Therefore, β is restricted to be a linear combination of the rows in H: $\beta = H^T\alpha(\alpha \in R^{N\times m})$. In this way, the following equation can be gotten as:

$$\beta^* = H^T\left(H^TH + \frac{I}{C}\right)^{-1} T \tag{16}$$

thus, the results of the RELM are represented as:

$$f_L(x) = \sum_{i=1}^{N} \beta_i^* g(a_i,b_i,x_i) \tag{17}$$

In this study, the components of the input matrix and the training data target matrix are normalized to [−1,1], a is set to 0. $C$and $b$are both optimized by the GWO.

2.4. Grey wolf optimizer

The GWO proposed by Mirjalili et al. [40] is a meta-heuristic, which was inspired by the hunting structure and the leadership hierarchy of grey wolves in nature. As proposed in Ref. [40], the encircling behavior of a grey wolf during hunting can be modeled as follows:

Table 5
The promoting percentages of the single RELM model by the GWO-RELM model for the wind speed series #1.

Indexes	GWO-RELM vs. RELM						
	1-step	2-step	3-step	4-step	5-step	6-step	7-step
P_{MAPE} (%)	0.71	2.28	1.12	1.55	1.35	3.27	0.77
P_{MAE} (%)	1.52	5.00	1.55	1.53	0.65	2.76	0.47
P_{RMSE} (%)	3.29	4.82	2.91	4.93	2.37	2.68	1.91
P_{SDE} (%)	3.85	8.34	3.96	5.89	0.15	-0.70	-0.46

Table 6
The promoting percentages of the single RELM model by the hybrid GWO-RELM model for the wind speed series #2.

Indexes	GWO-RELM vs. RELM						
	1-step	2-step	3-step	4-step	5-step	6-step	7-step
P_{MAPE} (%)	3.46	3.13	2.90	3.44	0.59	1.33	2.67
P_{MAE} (%)	4.54	4.05	3.81	4.97	2.62	3.62	6.03
P_{RMSE} (%)	3.68	2.53	3.79	4.31	4.48	4.17	2.83
P_{SDE} (%)	3.72	2.55	3.67	4.16	4.11	3.45	1.40

Table 7
The promoting percentages of the single RELM model by the hybrid GWO-RELM model for the wind speed series #3.

Indexes	GWO-RELM vs. RELM						
	1-step	2-step	3-step	4-step	5-step	6-step	7-step
P_{MAPE} (%)	10.32	3.18	5.14	1.38	4.50	7.93	7.36
P_{MAE} (%)	11.10	4.50	6.32	2.77	5.32	8.18	7.39
P_{RMSE} (%)	8.86	7.84	7.37	4.26	7.30	8.94	7.58
P_{SDE} (%)	6.48	5.96	4.79	0.01	5.55	8.41	7.18

Table 8
The promoting percentages of the single RELM model by the hybrid GWO-RELM model for the wind speed series #4.

Indexes	GWO-RELM vs. RELM						
	1-step	2-step	3-step	4-step	5-step	6-step	7-step
P_{MAPE} (%)	0.30	4.06	1.85	3.39	6.19	8.82	10.97
P_{MAE} (%)	−0.80	4.18	3.30	2.16	5.36	7.72	9.79
P_{RMSE} (%)	0.72	−1.13	3.67	−1.03	4.21	7.34	10.35
P_{SDE} (%)	1.18	−0.99	3.23	−0.75	4.07	7.46	10.35

Table 9
The promoting percentages of the hybrid EWT-RELM-IEWT model by the hybrid EWT-GWO-RELM-IEWT model for the wind speed series #1.

Indexes	EWT-GWO-RELM-IEWT vs. EWT-RELM-IEWT						
	1-step	2-step	3-step	4-step	5-step	6-step	7-step
P_{MAPE} (%)	83.59	78.81	77.94	73.25	69.98	65.98	63.60
P_{MAE} (%)	82.73	77.88	76.84	71.89	68.53	64.56	62.00
P_{RMSE} (%)	83.10	77.61	76.56	71.96	68.81	63.26	62.08
P_{SDE} (%)	82.66	76.19	74.81	69.34	67.42	60.49	58.52

$$\overrightarrow{D} = |\overrightarrow{C}.\ \overrightarrow{X_p}(t) - \overrightarrow{X}(t)| \tag{18}$$

$$\overrightarrow{X}(t+1) = \overrightarrow{X_p}(t) - \overrightarrow{A}\ .\ \overrightarrow{D} \tag{19}$$

where $\overrightarrow{X_p}(t)$ and $\overrightarrow{X}(t)$ indicate the position vector of the prey and the position vector of a grey wolf, respectively. $\overrightarrow{C}$ and $\overrightarrow{A}$ are coefficient vectors which can be calculated as follows:

$$\overrightarrow{A} = 2\overrightarrow{a}.\ \overrightarrow{r_1} - \overrightarrow{a} \tag{20}$$

$$\overrightarrow{C} = 2.\ \overrightarrow{r_2} \tag{21}$$

where elements of $\overrightarrow{a}$ are linearly decreased from 2 to 0 in iterations, and $\overrightarrow{r_1}$, $\overrightarrow{r_2}$ are random vectors whose components are randomly generated from [0,1]. In other words, $\overrightarrow{A}$ is a random value in the interval $[-a,a]$ where a is decreased from 2 to 0 over the course of iterations. It can be inferred from (19) that if $|A| < 1$, $\overrightarrow{X}(t+1)$ can be in any position between $\overrightarrow{X_p}(t)$ and $\overrightarrow{X}(t)$, which models the attacking prey. And $|A| > 1$ in initial iteration is designed to force the grey wolves to diverge from the current prey and search for a better one. Besides, the $\overrightarrow{C}$ is another component to favor exploration and avoid local optima. It works by deemphasizing ($|C| < 1$) the effect of the current prey, which proved to be very helpful when it stuck in local optima, especially in the last several iterations.

Apart from the hunting mechanism of a single grey wolf, the leadership hierarchy is another important component of the GWO. As defined in Ref. [40], there are three kinds of ranking grey wolves in group, in which the best solution are considered as the alpha (α), the second and third fittest solutions are named beta (β) and delta (δ), respectively. The rest wolves in the group are omega (ω), which are guided by the ranking grey wolves during hunting. It is supposed that the ranking wolves have more knowledge about the possible locations of the prey, so the positions of the search agents can be updated as follows [40]:

$$\overrightarrow{D_\alpha} = |\overrightarrow{C_1}.\ \overrightarrow{X_\alpha} - \overrightarrow{X}| \tag{22}$$

$$\overrightarrow{D_\beta} = |\overrightarrow{C_2}.\ \overrightarrow{X_\beta} - \overrightarrow{X}| \tag{23}$$

$$\overrightarrow{D_\delta} = |\overrightarrow{C_3}.\ \overrightarrow{X_\delta} - \overrightarrow{X}| \tag{24}$$

$$\overrightarrow{X_1} = \overrightarrow{X_\alpha} - \overrightarrow{A_1}\ .\ \overrightarrow{D_\alpha} \tag{25}$$

$$\overrightarrow{X_2} = \overrightarrow{X_\beta} - \overrightarrow{A_2}\ .\ \overrightarrow{D_\beta} \tag{26}$$

$$\overrightarrow{X_3} = \overrightarrow{X_\delta} - \overrightarrow{A_3}\ .\ \overrightarrow{D_\delta} \tag{27}$$

$$\overrightarrow{X}(t+1) = \frac{1}{3}(\overrightarrow{X_1} + \overrightarrow{X_2} + \overrightarrow{X_3}) \tag{28}$$

The pseudo code of the GWO algorithm can be given as follows:

Objective function	$f(X)$, $X_i = (X_{i1}, X_{i2} ... X_{in})$,
Parameters:	
i	*iteration number*
M	the maximum number of iterations
N	the number of wolves in the group
1.	Initialize the grey wolf group $X_j (i = 1,2,...,M)$,
2.	Calculate the fitness of each search agent
3.	X_α = *the best search agent*
4.	X_β = *the second best search agent*
5.	X_δ = *the third best search agent*
6.	***for*** $i = 1$ *to M*
7.	***for*** $j = 1$ *to N*
8.	Generate A_1,A_2,A_3,C_1,C_2 *and* C_3 according to (20) and (21)
9.	Update the position of the current search agents according to Eq. (28)
10.	***end for***
11.	Calculate the fitness of all search agents
12.	X_α = *the best search agent*
13.	X_β = *thesecond best search agent*
14.	X_δ = *the third best search agent*

Table 10
The promoting percentages of the hybrid EWT-RELM-IEWT model by the hybrid EWT-GWO-RELM-IEWT model for the wind speed series #2.

Indexes	EWT-GWO-RELM-IEWT vs. EWT-RELM-IEWT						
	1-step	2-step	3-step	4-step	5-step	6-step	7-step
P_{MAPE} (%)	80.92	78.70	76.46	73.89	70.81	68.73	67.70
P_{MAE} (%)	80.80	78.60	76.38	73.87	70.88	68.88	67.83
P_{RMSE} (%)	81.90	78.95	76.74	74.09	71.35	68.92	67.75
P_{SDE} (%)	81.82	78.63	75.95	72.62	69.02	65.58	63.41

Table 11
The promoting percentages of the hybrid EWT-RELM-IEWT model by the hybrid EWT-GWO-RELM-IEWT model for the wind speed series #3.

Indexes	EWT-GWO-RELM-IEWT vs. EWT-RELM-IEWT						
	1-step	2-step	3-step	4-step	5-step	6-step	7-step
P_{MAPE} (%)	82.86	79.76	71.55	72.18	68.60	65.81	61.92
P_{MAE} (%)	83.20	79.96	72.00	72.34	68.88	66.20	62.28
P_{RMSE} (%)	82.60	78.72	70.46	70.88	67.13	64.37	60.64
P_{SDE} (%)	81.07	76.25	64.42	66.99	60.99	59.62	56.41

Table 12
The promoting percentages of the hybrid EWT-RELM-IEWT model by the hybrid EWT-GWO-RELM-IEWT model for the wind speed series #4.

Indexes	EWT-GWO-RELM-IEWT vs. EWT-RELM-IEWT						
	1-step	2-step	3-step	4-step	5-step	6-step	7-step
P_{MAPE} (%)	74.80	66.20	47.30	51.11	46.83	47.55	46.11
P_{MAE} (%)	75.05	66.55	47.80	51.56	47.62	48.81	47.23
P_{RMSE} (%)	74.93	66.53	47.20	52.35	48.02	49.81	48.41
P_{SDE} (%)	74.46	65.92	45.92	51.19	46.65	48.64	47.65

Table 13
The promoting percentages of the hybrid GWO-EWT-RELM model by the hybrid EWT-GWO-RELM-IEWT model for the wind speed series #1.

Indexes	EWT-GWO-RELM-IEWT vs. GWO-EWT-RELM						
	1-step	2-step	3-step	4-step	5-step	6-step	7-step
P_{MAPE} (%)	68.77	52.10	47.28	38.48	28.43	19.93	14.80
P_{MAE} (%)	68.62	52.07	46.82	38.25	28.32	19.58	13.84
P_{RMSE} (%)	69.80	53.13	47.42	38.00	30.87	19.15	15.07
P_{SDE} (%)	70.50	53.81	48.99	39.42	36.23	21.82	17.13

Table 14
The promoting percentages of the hybrid GWO-EWT-RELM model by the hybrid EWT-GWO-RELM-IEWT model for the wind speed series #2.

Indexes	EWT-GWO-RELM-IEWT vs. GWO-EWT-RELM						
	1-step	2-step	3-step	4-step	5-step	6-step	7-step
P_{MAPE} (%)	54.52	47.07	39.69	33.67	30.61	25.05	21.97
P_{MAE} (%)	54.81	47.35	39.76	33.45	30.89	24.61	21.77
P_{RMSE} (%)	56.03	48.53	41.99	36.11	34.05	26.52	23.36
P_{SDE} (%)	56.03	48.54	42.03	36.15	34.11	26.49	23.34

15. ***end for***
16. return X_α

As shown in the algorithm, there are several components to be determined in the GWO. In this study, the parameters of the RELM are regarded as the optimization variables: $X = (C,b)$, in which $C \in [2^{-8},2^{8}]$,$b \in [2^{-5},2^{5}]$; $f(X)$ are equal to the root mean square error of the validation set; the maximum number of iterations and the number of wolves in the group are equal to 30 and 20, respectively.

Table 15
The promoting percentages of the hybrid GWO-EWT-RELM model by the hybrid EWT-GWO-RELM-IEWT model for the wind speed series #3.

Indexes	EWT-GWO-RELM-IEWT vs. GWO-EWT-RELM						
	1-step	2-step	3-step	4-step	5-step	6-step	7-step
P_{MAPE} (%)	34.07	27.76	10.04	17.05	24.04	23.34	16.57
P_{MAE} (%)	32.14	25.59	7.96	14.11	21.77	22.12	14.64
P_{RMSE} (%)	32.51	24.06	6.18	11.31	18.79	22.26	15.14
P_{SDE} (%)	37.23	29.09	6.08	13.11	21.42	29.59	22.72

Table 16
The promoting percentages of the hybrid GWO-EWT-RELM model by the hybrid EWT-GWO-RELM-IEWT model for the wind speed series #4.

Indexes	EWT-GWO-RELM-IEWT vs. GWO-EWT-RELM						
	1-step	2-step	3-step	4-step	5-step	6-step	7-step
P_{MAPE} (%)	66.29	48.06	16.02	21.67	11.24	15.21	11.02
P_{MAE} (%)	66.42	48.36	16.64	22.58	12.09	16.86	12.16
P_{RMSE} (%)	66.09	49.36	16.23	26.88	14.95	19.21	14.69
P_{SDE} (%)	66.41	49.74	16.30	26.96	14.99	19.32	14.83

Table 17
The promoting percentages of the hybrid GWO-EWT-SVM-IEWT model by the hybrid EWT-GWO-RELM-IEWT model for the wind speed series #1.

Indexes	EWT-GWO-RELM-IEWT vs. EWT-GWO-SVM-IEWT						
	1-step	2-step	3-step	4-step	5-step	6-step	7-step
P_{MAPE} (%)	89.49	84.40	82.65	78.68	73.41	65.54	58.29
P_{MAE} (%)	88.88	83.81	81.88	77.83	72.44	64.46	56.69
P_{RMSE} (%)	89.41	83.08	81.19	77.89	72.72	63.44	57.66
P_{SDE} (%)	89.27	81.01	77.10	71.41	65.09	52.85	48.98

Table 18
The promoting percentages of the hybrid GWO-EWT-SVM-IEWT model by the hybrid EWT-GWO-RELM-IEWT model for the wind speed series #2.

Indexes	EWT-GWO-RELM-IEWT vs. EWT-GWO-SVM-IEWT						
	1-step	2-step	3-step	4-step	5-step	6-step	7-step
P_{MAPE} (%)	83.24	78.52	75.58	74.39	68.09	66.60	65.46
P_{MAE} (%)	83.41	78.46	75.41	74.76	67.32	65.84	66.27
P_{RMSE} (%)	84.18	78.85	76.52	75.36	67.90	65.23	66.59
P_{SDE} (%)	84.13	78.84	75.53	72.50	67.99	65.31	58.24

Table 19
The promoting percentages of the hybrid GWO-EWT-SVM-IEWT model by the hybrid EWT-GWO-RELM-IEWT model for the wind speed series #3.

Indexes	EWT-GWO-RELM-IEWT vs. EWT-GWO-SVM-IEWT						
	1-step	2-step	3-step	4-step	5-step	6-step	7-step
P_{MAPE} (%)	82.43	76.13	61.35	58.29	52.59	45.91	36.63
P_{MAE} (%)	82.82	76.43	61.90	58.24	52.33	45.72	36.51
P_{RMSE} (%)	81.73	74.38	58.27	55.26	49.29	43.07	34.40
P_{SDE} (%)	73.45	64.71	40.28	45.22	38.93	36.55	28.11

2.5. Performance evaluation indexes

In order to offer an objective assessment of the involved models, several metrics are used in this study. There are the Mean Absolute Error (MAE), including the Mean Absolute Percentage Error (MAPE),

Table 20
The promoting percentages of the hybrid GWO-EWT-SVM-IEWT model by the hybrid EWT-GWO-RELM-IEWT model for the wind speed series #4.

Indexes	EWT-GWO-RELM-IEWT vs. EWT-GWO-SVM-IEWT						
	1-step	2-step	3-step	4-step	5-step	6-step	7-step
P_{MAPE} (%)	78.39	61.52	24.00	27.65	24.53	31.81	33.83
P_{MAE} (%)	78.40	61.31	24.39	27.58	24.25	32.02	33.92
P_{RMSE} (%)	78.20	62.02	26.19	28.34	24.57	34.29	36.78
P_{SDE} (%)	78.30	61.09	18.84	25.62	21.58	32.30	36.17

the Root Mean Square Error (RMSE), the Standard Deviation of Error (SDE), the Promoting Percentages of Mean Absolute Error (P_{MAE}), the Promoting Percentages of Mean Absolute Percentage Error (P_{MAPE}), the Promoting Percentages of Root Mean Square error (P_{RMSE}), the Promoting percentages of Standard Deviation of Error (P_{SDE}). The equations of these evaluation indexes are explained as follows:

$$\begin{cases} MAE = (\sum_{t=1}^{N} |X(t)-\hat{X}(t)|)/N \\ MAPE = (\sum_{t=1}^{N} |(X(t)-\hat{X}(t))/X(t)|)/N \\ RMSE = \sqrt{(\sum_{t=1}^{N} [X(t)-\hat{X}(t)]^2)/N} \\ SDE = \sqrt{(\sum_{t=1}^{N} \left[X(t)-\hat{X}(t)-\sum_{t=1}^{N} (X(t)-\hat{X}(t))/N\right]^2)/N} \end{cases} \tag{29}$$

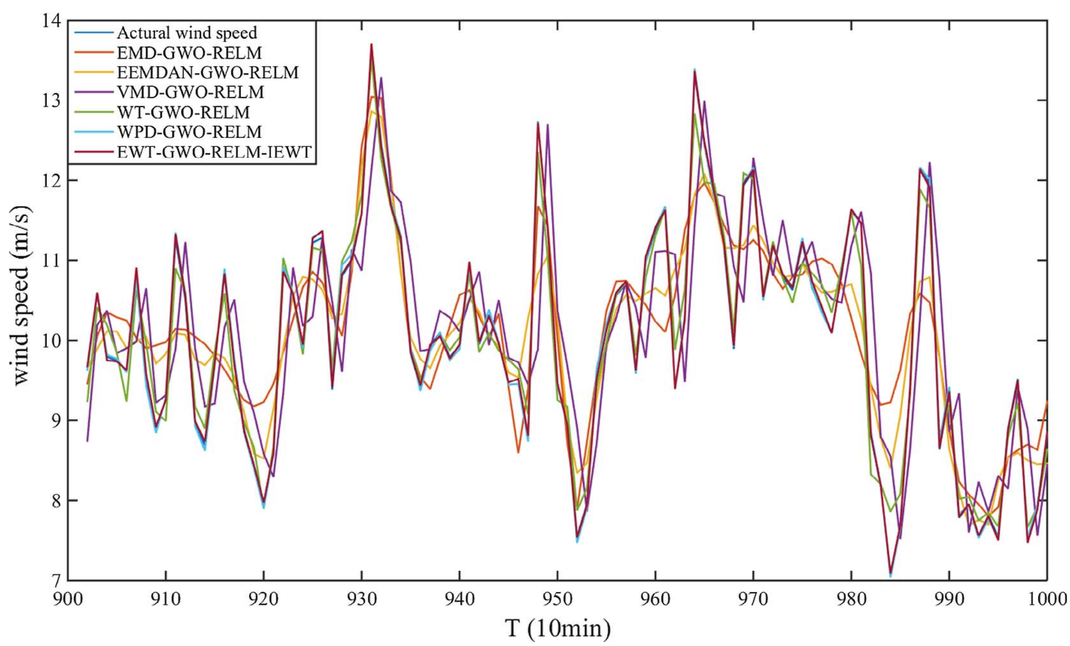

Fig. 7. The results of the one-step predictions for the wind speed series #1.

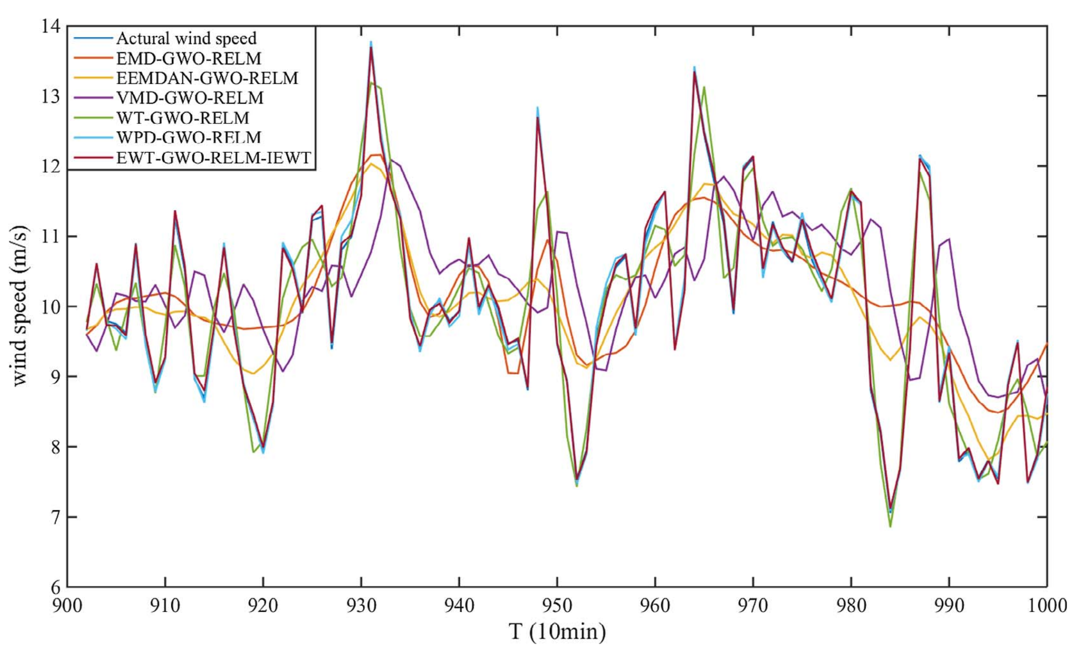

Fig. 8. The results of the two-step predictions for the wind speed series #1.

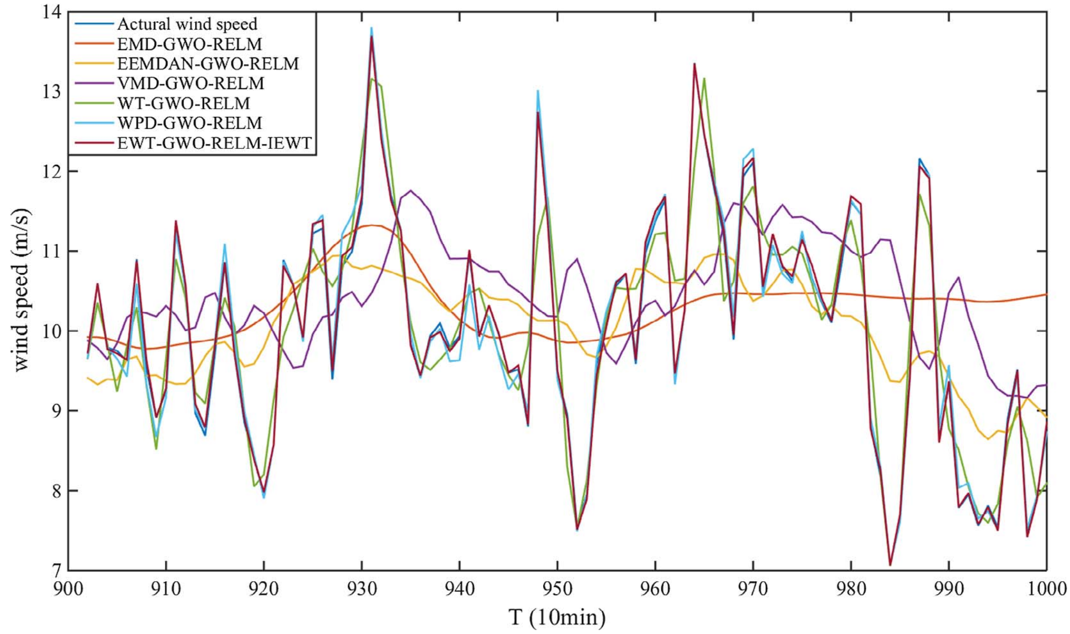

Fig. 9. The results of the three-step predictions for the wind speed series #1.

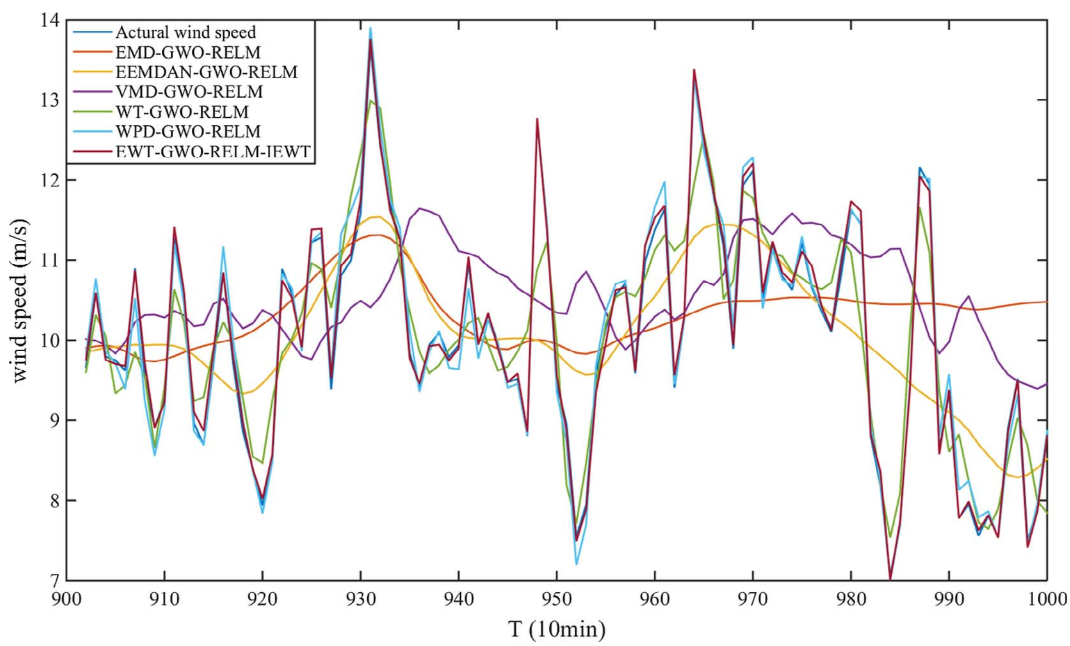

Fig. 10. The results of the four-step predictions for the wind speed series #1.

$$\begin{cases} P_{\mathrm{MAE}} = |MAE_1 - MAE_2|/MAE_1 \\ P_{\mathrm{MAPE}} = |MAPE_1 - MAPE_2|/MAPE_1 \\ P_{RMSE} = |RMSE_1 - RMSE_2|/RMSE_1 \\ P_{SDE} = |SDE_1 - SDE_2|/SDE_1 \end{cases} \tag{30}$$

where $X(t)$ represents the wind speed series, $\hat{X}(t)$ represents the forecasted values, and N implicates the number of $X(t)$.

3. Case study

3.1. Wind speed time series

Four wind speed series from wind farm in China are adopted in this study to validate the forecasting capacity of the proposed model. The shape of the wind speed series are shown in Figs. 3–6. There are a total of 1000 samples in each series, which are separated into the training set, the validation set and the testing set. The training set is used to train the RELM model. The validation set is adopted to find the suitable parameters of the RELM model with the promotion of the GWO. The testing set is used to check the forecasting performance of the constructed models.

3.2. Experiments

To evaluate the prediction performance of the proposed hybrid EWT-GWO-RELM-IEWT model, ten different forecasting models are included in the comparison of the forecasting results. The involved forecasting models consist of the RELM model, the hybrid GWO-RELM model, the hybrid EWT-RELM-IEWT model, the hybrid EWT-GWO-RELM model, the hybrid EWT-GWO-SVM-IEWT model, the hybrid

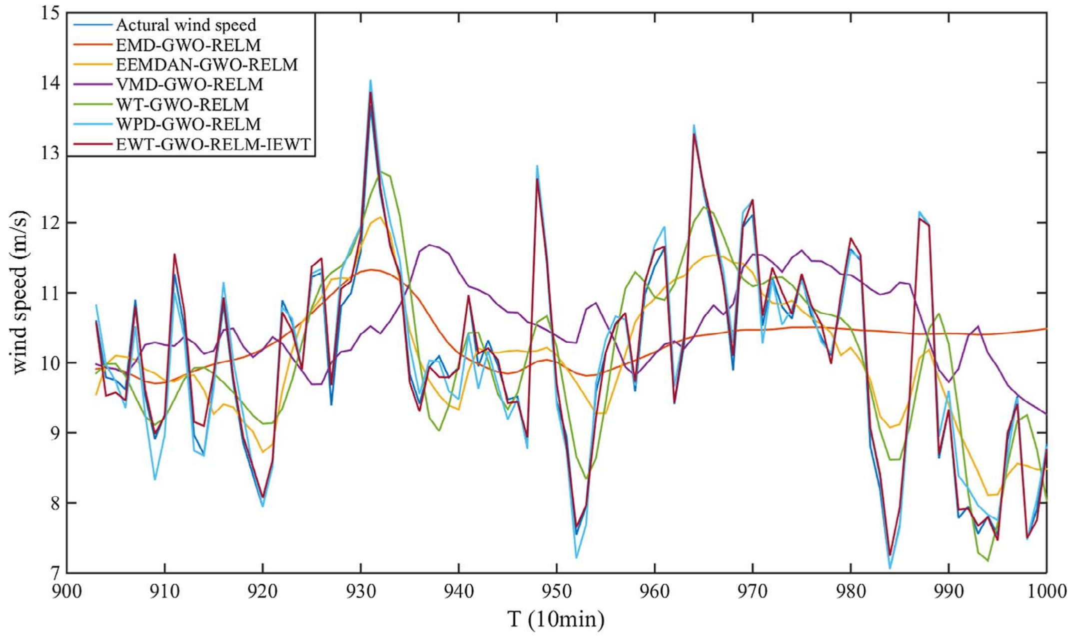

Fig. 11. The results of the five-step predictions for the wind speed series #1.

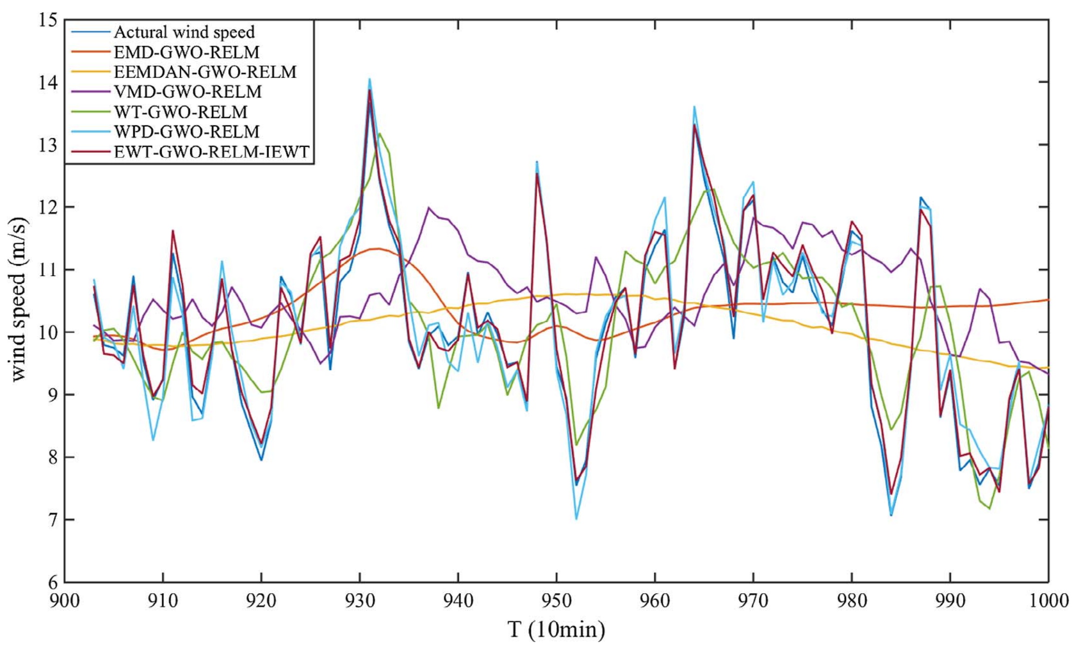

Fig. 12. The results of the six-step predictions for the wind speed series #1.

VMD-GWO-RELM model, the hybrid EMD-GWO-RELM model, the hybrid EEMDAN-GWO-RELM model, the hybrid WT-GWO-RELM model and the hybrid WPD-GWO-RELM model. The error estimated results of different forecasting models are provided in Tables 1–4.

3.3. Comparison and analysis

Tables 5–8 display the comparing results between the hybrid GWO-RELM model and the single RELM model in the four experimental series. Tables 9–12 give the comparing results between the hybrid EWT-GWO-RELM-IEWT model and the hybrid EWT-RELM-IEWT model. Tables 13–16 show the comparing results between the hybrid EWT-GWO-RELM-IEWT and the hybrid GWO-EWT-RELM model. Tables 17–20 illustrate the comparing results between the hybrid EWT-GWO-RELM-IEWT model and the hybrid EWT-GWO-SVM-IEWT model. Figs. 7–17 show the forecasting results of several forecasting models with different decomposing techniques in the proposed hybrid structure. Tables 21–24 give the comparing results between the hybrid EWT-GWO-RELM-IEWT model and the hybrid WPD-GWO- RELM model.

From Tables 1–24 and Figs. 7–17, it can be found that:

(1) When comparing the hybrid GWO-RELM model with the single RELM model, the former has not improved the performance of the latter considerably. For instance, in the case one, in 1-step, 3-step, 5-step and 7-step predictions, the MAPE promoting percentages by the GWO component are 0.71%, 1.12%, 1.35% and 0.77%, respectively; the MAE promoting percentages by the GWO component are 1.52%, 1.55%, 0.65% and 0.47%, respectively; the RMSE promoting percentages by the GWO component are 3.29%, 2.91%, 2.37% and 1.91%, respectively; and the SDE promoting percentages by the GWO

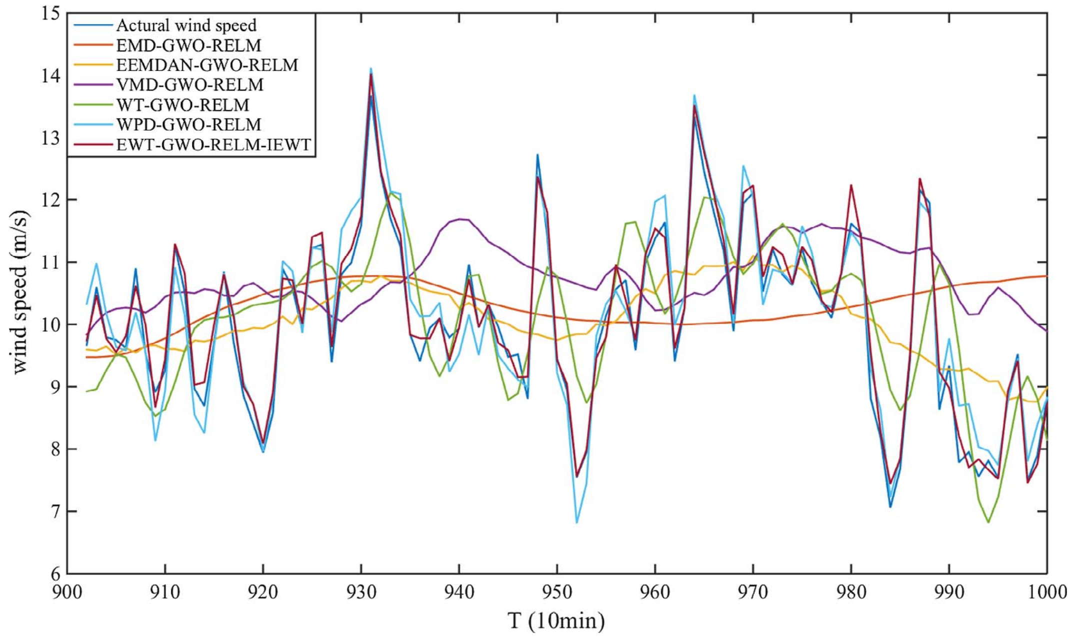

Fig. 13. The results of the seven-step predictions for the wind speed series #1.

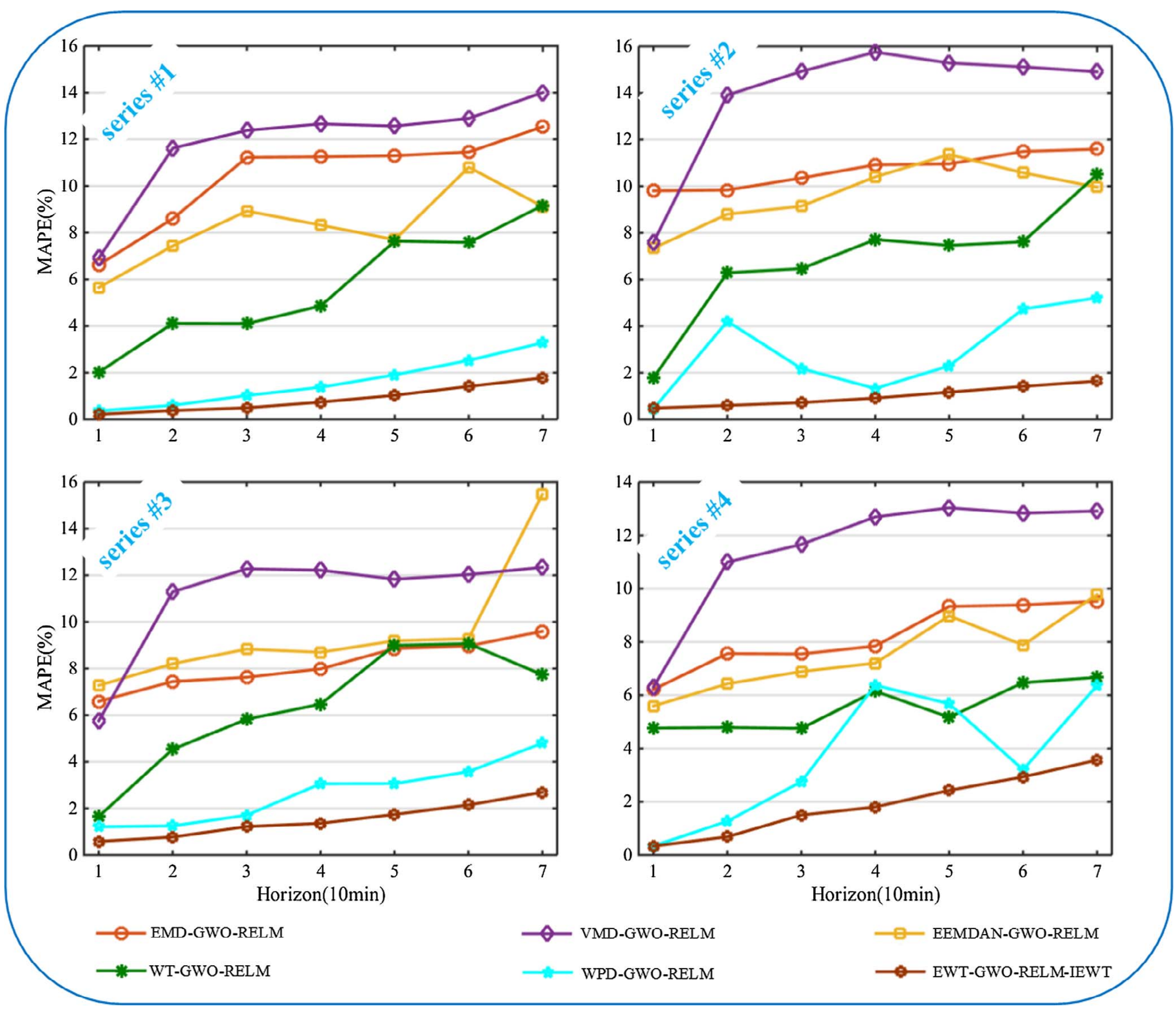

Fig. 14. The estimated MPAE results of the involved models for the multistep predictions.

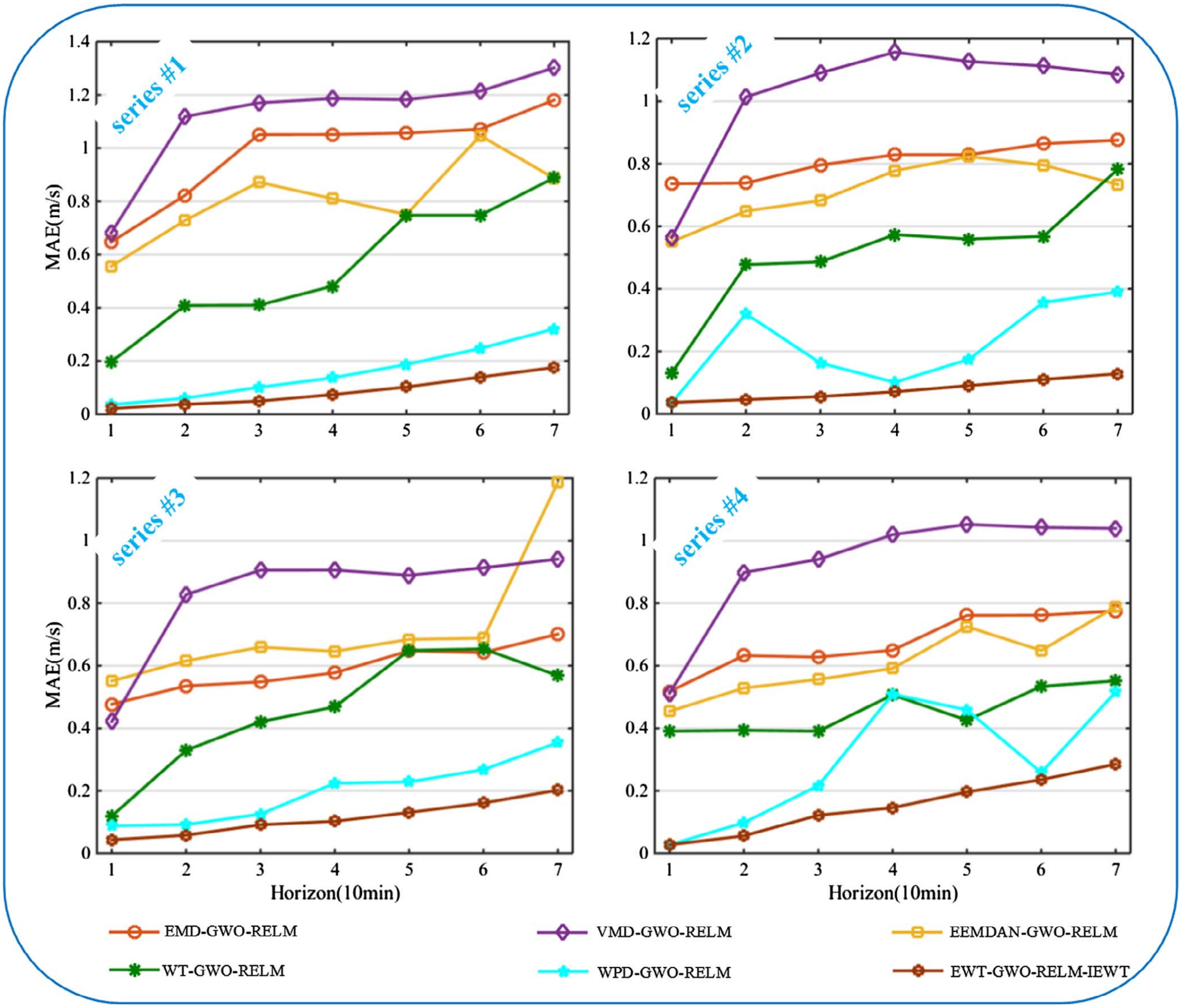

Fig. 15. The estimated MAE results of the involved models for the multistep predictions.

component are 3.85%, 3.96%, 0.15% and -0.46%, respectively.

(2) When comparing the hybrid EWT-GWO-RELM-IEWT model with the hybrid EWT-RELM-IEWT model, the GWO has improved the performance of the hybrid EWT-RELM-IEWT model significantly. For instance, in the case one, in 1-step, 3-step, 5-step and 7-step predictions, the MAPE promoting percentages by the GWO component are 83.59%, 77.94%, 69.98% and 63.60%, respectively; the MAE promoting percentages by the GWO component are 82.73%, 76.84%, 68.53% and 62.00%, respectively; the RMSE promoting percentages by the GWO component are 83.10%, 76.56%, 68.81% and 62.08%, respectively; and the SDE promoting percentages by the GWO component are 82.66%, 74.81%, 67.42% and 58.52%, respectively.

(3) The prediction accuracy and stability of the hybrid EWT-GWO-RELM-IEWT model are better than that of the hybrid EWT-GWO-RELM model. For instance, in the case one, in 1-step, 3-step, 5-step and 7-step predictions, the MAPE promoting percentages by the IEWT component are 68.77%, 47.28%, 28.43% and 14.80%, respectively; the MAE promoting percentages by the IEWT component are 68.62%, 46.82%, 28.32% and 13.84%, respectively; the RMSE promoting percentages by the IEWT component are 69.80%, 47.42%, 30.87% and 15.07%, respectively; and the SDE promoting percentages by the IEWT component are 70.50%, 48.99%, 36.23% and 17.13%, respectively.

(4) The prediction accuracy and stability of the hybrid EWT-GWO-RELM-IEWT model are better than that of the hybrid EWT-GWO-SVM-IEWT model. For instance, in the case one, in 1-step, 3-step, 5-step and 7-step predictions, the MAPE promoting percentages of the hybrid EWT-GWO-SVM-IEWT model by the hybrid EWT-GWO-RELM-IEWT model are 89.49%, 82.65%, 73.41% and 58.29%, respectively; the MAE promoting percentages of the hybrid EWT-GWO-SVM-IEWT model by the hybrid EWT-GWO-RELM-IEWT model are 88.88%, 81.88%, 72.44% and 56.69%, respectively; the RMSE promoting percentages of the hybrid EWT-GWO-SVM-IEWT model by the hybrid EWT-GWO-RELM-IEWT model are 89.41%, 81.19%, 72.72% and 57.66%, respectively; and the SDE promoting percentages of the hybrid EWT-GWO-SVM-IEWT model by the hybrid EWT-GWO-RELM-IEWT model are 89.27%, 77.10%, 65.09% and 48.98%, respectively. The RELM is more suitable than the SVM in the proposed hybrid EWT-GWO-IEWT structure.

(5) The prediction accuracy and stability of the hybrid EWT-GWO-RELM-IEWT model are better than that of the hybrid VMD-GWO-RELM model, the hybrid EMD-GWO-RELM model, the hybrid EEMDAN-GWO-RELM model and the hybrid WT-GWO-RELM

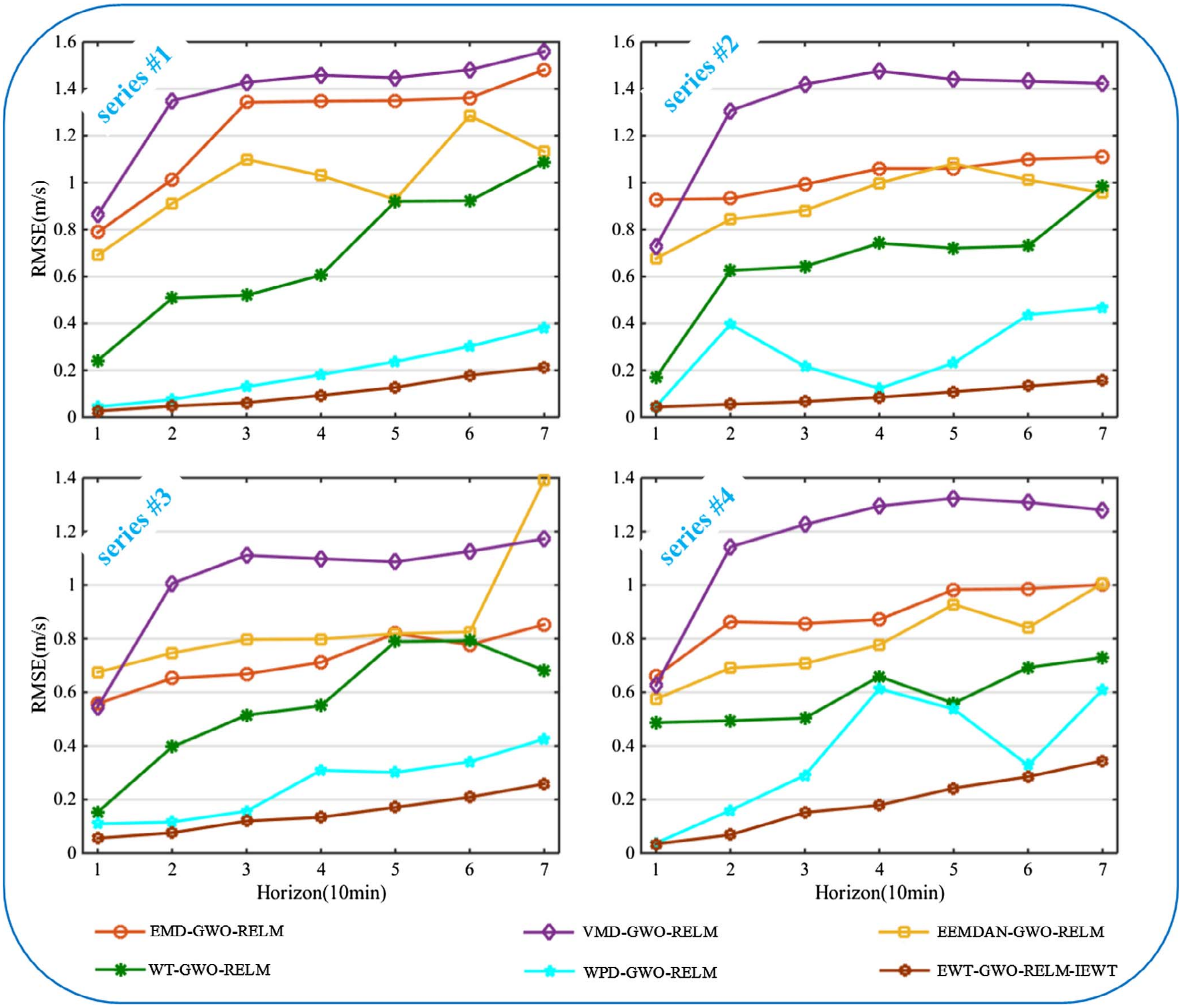

Fig. 16. The estimated RMSE results of the involved models for the multistep predictions.

model. As shown in Figs. 13-16, the MAPE, the MAE, the RMSE and the SDE of the hybrid EWT-GWO-RELM-IEWT are small than that of the aforementioned wind speed prediction models in all horizon and case. Among the included data decomposing algorithms, the EWT is the most suitable in the proposed forecasting and optimizing structure.

(6) The multistep prediction accuracy and stability of the hybrid EWT-GWO-RELM-IEWT model are better than that of the hybrid WPD-GWO-RELM model. For instance, in the case one, from 2-step to 7-step predictions, the MAPE promoting percentages of the hybrid WPD-GWO-RELM model by the hybrid EWT-GWO-RELM-IEWT model are 51.85%, 46.35%, 46.03%, 44.03% and 45.90%, respectively; the MAE promoting percentages of the hybrid WPD-GWO-RELM model by the hybrid EWT-GWO-RELM-IEWT model are 51.36%, 45.97%, 45.20%, 43.51% and 45.22%, respectively; the RMSE promoting percentages of the hybrid WPD-GWO-RELM model by the hybrid EWT-GWO-RELM-IEWT model are 36.59%, 52.27%, 48.72%, 46.34%, 40.80% and 44.30%, respectively; and the SDE promoting percentages of the hybrid WPD-GWO-RELM model by the hybrid EWT-GWO-RELM-IEWT model are 53.19%, 49.47%, 49.99%, 43.32% and 45.94%, respectively.

(7) The hybrid EWT-GWO-RELM-IEWT model and hybrid WPD-GWO-RELM model have similar performance in the 1-step predictions in some cases. For instance, in the case two, the MAPE promoting percentage, the MAE promoting percentage, the RMSE promoting percentage and the SDE promoting percentage of the hybrid WPD-GWO-RELM model by the hybrid EWT-GWO-RELM-IEWT model are −0.63%, −3.54%, 4.08% and 4.07%, respectively.

4. Conclusions

In this study, a novel model is proposed based on the EWT decomposition, the GWO algorithm, the RELM network and the IEWT reconstruction. The EWT is adopted to decompose the raw series into several subseries adaptively. The RELM network optimized by GWO algorithm is employed to forecast each subseries. The IEWT, which acts as a filter bank, is used to reconstruct the combined subseries. To evaluate the performance of the proposed model, different forecasting models are implemented on four series. The included forecasting models consist of the single RELM model, the hybrid GWO-RELM model, the hybrid EWT-RELM-IEWT model, the hybrid EWT-GWO-RELM model, the hybrid EWT-GWO-SVM-IEWT model, the hybrid VMD-GWO-RELM model, the hybrid EMD-GWO-RELM model, the hybrid EEMDAN-GWO-RELM model, the hybrid WT-GWO-RELM model

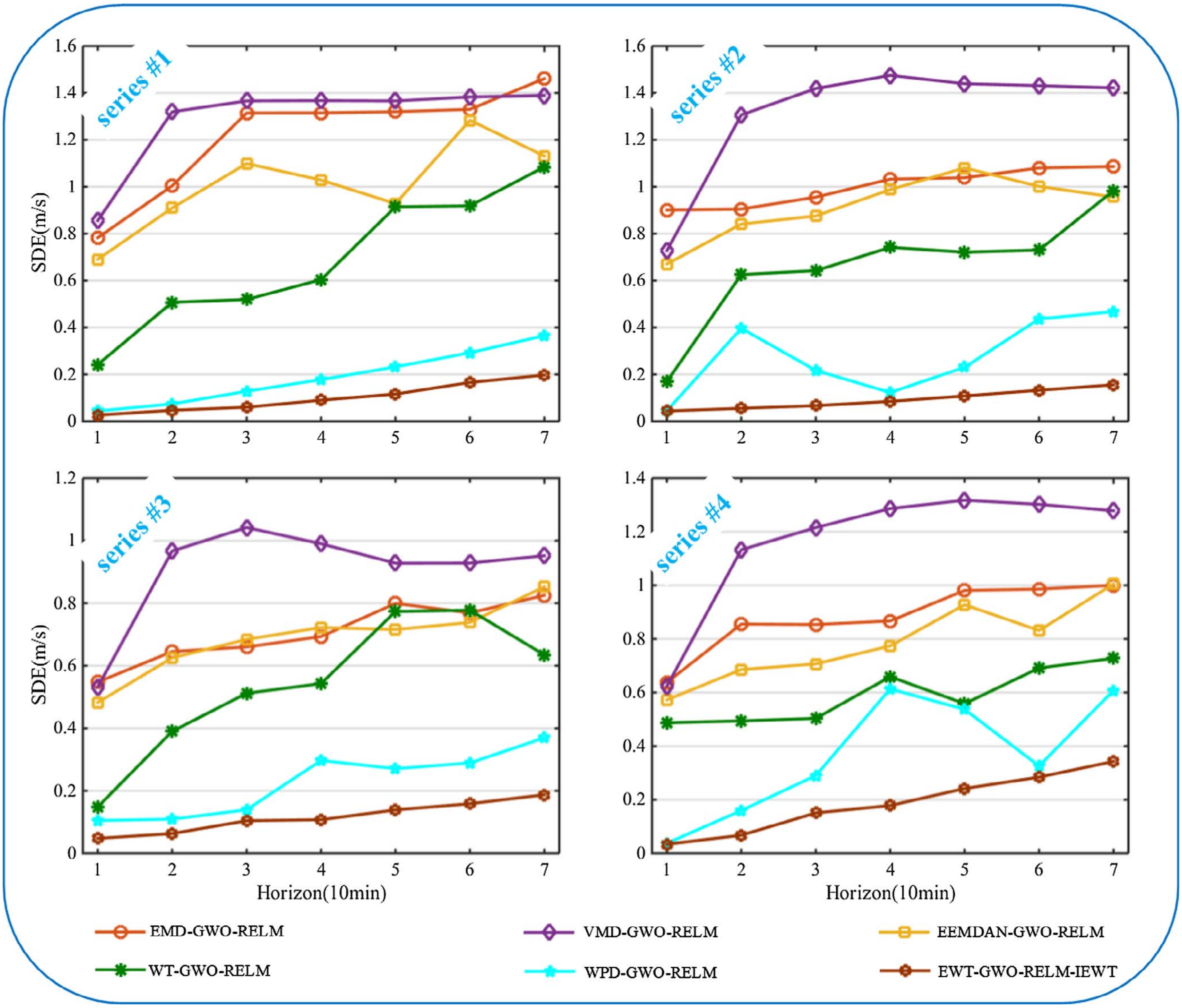

Fig. 17. The estimated SDE results of the involved models for the multistep predictions.

Table 21
The promoting percentages of the hybrid GWO-WPD-RELM model by the hybrid EWT-GWO-RELM-IEWT model for the wind speed series #1.

Indexes	EWT-GWO-RELM-IEWT vs. EWT-WPD-RELM						
	1-step	2-step	3-step	4-step	5-step	6-step	7-step
P_{MAPE} (%)	41.53	37.40	51.85	46.35	46.03	44.03	45.90
P_{MAE} (%)	41.18	38.27	51.36	45.97	45.20	43.51	45.22
P_{RMSE} (%)	40.14	36.59	52.27	48.72	46.34	40.80	44.30
P_{SDE} (%)	40.28	36.68	53.19	49.47	49.99	43.32	45.94

Table 22
The promoting percentages of the hybrid GWO-WPD-RELM model by the hybrid EWT-GWO-RELM-IEWT model for the wind speed series #2.

Indexes	EWT-GWO-RELM-IEWT vs. EWT-WPD-RELM						
	1-step	2-step	3-step	4-step	5-step	6-step	7-step
P_{MAPE} (%)	−6.03	85.81	67.03	31.21	49.13	70.08	68.49
P_{MAE} (%)	−3.54	85.77	65.89	30.05	48.18	69.17	67.11
P_{RMSE} (%)	4.08	86.07	69.36	30.90	53.13	69.56	66.60
P_{SDE} (%)	4.07	86.07	69.38	30.99	53.21	69.63	66.71

Table 23
The promoting percentages of the hybrid GWO-WPD-RELM model by the hybrid EWT-GWO-RELM-IEWT model for the wind speed series #3.

Indexes	EWT-GWO-RELM-IEWT vs. EWT-WPD-RELM						
	1-step	2-step	3-step	4-step	5-step	6-step	7-step
P_{MAPE} (%)	51.75	38.35	28.66	55.50	43.10	39.88	43.97
P_{MAE} (%)	50.77	36.94	27.47	54.24	42.69	39.91	42.97
P_{RMSE} (%)	49.09	34.66	23.50	56.68	43.19	38.71	39.28
P_{SDE} (%)	54.51	42.16	25.19	63.78	48.66	45.13	49.30

Table 24
The promoting percentages of the hybrid GWO-WPD-RELM model by the hybrid EWT-GWO-RELM-IEWT model for the wind speed series #4.

Indexes	EWT-GWO-RELM-IEWT vs. EWT-WPD-RELM						
	1-step	2-step	3-step	4-step	5-step	6-step	7-step
P_{MAPE} (%)	1.46	46.11	45.46	71.69	57.27	8.43	43.95
P_{MAE} (%)	-0.71	43.06	43.67	71.31	57.23	8.93	44.68
P_{RMSE} (%)	9.12	57.23	47.83	70.86	54.91	13.11	43.39
P_{SDE} (%)	10.04	57.69	47.98	70.94	54.96	12.78	43.56

and the hybrid WPD-GWO-RELM model. The experimental results of four metrics show that: (1) the IEWT is effective in improving the accuracy and stability of the wind speed predictions; (2) the GWO algorithm can promote the performance of the proposed EWT-RELM-IEWT forecasting structure significantly; (3) the performance of RELM network is better than the SVM in the proposed EWT-GWO-IEWT structure; and (4) the proposed hybrid model has the best multistep prediction performance compared with the other comparing models. The proposed hybrid model is suitable for the wind speed high-precision multistep forecasting.

Acknowledgements

This study is fully supported by the National Natural Science Foundation of China (Grant No. 51308553), the Changsha Science & Technology Project (Grant No. KQ1707017), the Shenghua Yu-ying Talents Program of the Central South University (Principle Investigator: Dr. Hui Liu), the innovation driven project of the Central South University (Project No. 502501002, Principle Investigator: Dr. Hui Liu), the engineering college 'double first-rate' supporting project of the Central South University and the Fundamental Research Funds for the Central Universities of Central South University. This study is partly supported by the National Natural Science Foundation of China (Grant No. U1534210, U1334205).

References

[1] Ouyang T, Zha X, Qin L. A combined multivariate model for wind power prediction. Energy Convers Manage 2017;144:361–73.
[2] Jung J, Broadwater RP. Current status and future advances for wind speed and power forecasting. Renew Sustain Energy Rev 2014;31(2):762–77.
[3] Kennedy J, Fox B, Morrow DJ. Distributed generation as a balancing resource for wind generation. IET Renew Power Gener 2007;1(3):167–74.
[4] Soman SS, Zareipour H, Malik O, et al. A review of wind power and wind speed forecasting methods with different time horizons. North American Power Symposium IEEE 2010:1–8.
[5] Zhao J, Guo Y, Xiao X, et al. Multi-step wind speed and power forecasts based on a WRF simulation and an optimized association method. Appl Energy 2017;197:183–202.
[6] Torres JL, García A, Blas MD, et al. Forecast of hourly average wind speed with ARMA models in Navarre (Spain). Sol Energy 2005;79(1):65–77.
[7] Li G, Shi J. On comparing three artificial neural networks for wind speed forecasting. Appl Energy 2010;87(7):2313–20.
[8] Liu H, Tian HQ, Li YF. Comparison of new hybrid FEEMD-MLP, FEEMD-ANFIS, wavelet packet-MLP and wavelet packet-ANFIS for wind speed predictions. Energy Convers Manage 2015;89:1–11.
[9] Tascikaraoglu A, Uzunoglu M. A review of combined approaches for prediction of short-term wind speed and power. Renew Sustain Energy Rev 2014;34(6):243–54.
[10] Yu C, Li Y, Zhang M. Comparative study on three new hybrid models using Elman neural network and empirical mode decomposition based technologies improved by singular spectrum analysis for hour-ahead wind speed forecasting. Energy Convers Manage 2017;147:75–85.
[11] Du P, Wang J, Guo Z, et al. Research and application of a novel hybrid forecasting system based on multi-objective optimization for wind speed forecasting. Energy Convers Manage 2017;150. 90-07.
[12] Wang Y, Wang J, Wei X. A hybrid wind speed forecasting model based on phase space reconstruction theory and Markov model: a case study of wind farms in northwest China. Energy 2015;91:556–72.
[13] Li H, Wang J, Lu H, et al. Research and application of a combined model based on variable weight for short term wind speed forecasting. Renew Energy 2018;116.
[14] Wang S, Zhang N, Wu L, et al. Wind speed forecasting based on the hybrid ensemble empirical mode decomposition and GA-BP neural network method. Renew Energy 2016;94:629–36.
[15] Sun W, Wang Y. Short-term wind speed forecasting based on fast ensemble empirical mode decomposition, phase space reconstruction, sample entropy and improved back-propagation neural network. Energy Convers Manage 2018;157:1–12.
[16] Zhang W, Qu Z, Zhang K, et al. A combined model based on CEEMDAN and modified flower pollination algorithm for wind speed forecasting. Energy Convers Manage 2017;136:439–51.
[17] Yu C, Li Y, Zhang M. An improved wavelet transform using singular spectrum analysis for wind speed forecasting based on elman neural network. Energy Convers Manage 2017;148:895–904.
[18] Liu H, Tian HQ, Li YF. Four wind speed multi-step forecasting models using extreme learning machines and signal decomposing algorithms. Energy Convers Manage 2015;100:16–22.
[19] Hu J, Wang J. Short-term wind speed prediction using empirical wavelet transform and Gaussian process regression. Energy 2015;93:1456–66.
[20] Hu J, Wang J, Ma K. A hybrid technique for short-term wind speed prediction. Energy 2015;81(1):563–74.
[21] Hu J, Wang J, Xiao L. A hybrid approach based on the Gaussian process with t -observation model for short-term wind speed forecasts. Renew Energy 2017;114:670–85.
[22] Liu H, Mi XW, Li YF. Wind speed forecasting method based on deep learning strategy using empirical wavelet transform, long short term memory neural network and Elman neural network. Energy Convers Manage 2017;156:498–514.
[23] Chang GW, Lu HJ, Chang YR, et al. An improved neural network-based approach for short-term wind speed and power forecast. Renew Energy 2017;105:301–11.
[24] Jiang P, Wang Y, Wang J. Short-term wind speed forecasting using a hybrid model. Energy 2016;119:561–77.
[25] Ren Y, Suganthan PN, Srikanth N. A novel empirical mode decomposition with support vector regression for wind speed forecasting. IEEE Trans Neural Networks & Learn Syst 2016;27(8):1793–8.
[26] Qu Z, Zhang K, Mao W, et al. Research and application of ensemble forecasting based on a novel multi-objective optimization algorithm for wind-speed forecasting. Energy Convers Manage 2017;154:440–54.
[27] Niu T, Wang J, Zhang K, et al. Multi-step-ahead wind speed forecasting based on optimal feature selection and a modified bat algorithm with the cognition strategy. Renew Energy 2017;143:410–30.
[28] Liu Hui, Mi Xiwei, Li Yanfei. Comparison of two new intelligent wind speed forecasting approaches based on wavelet packet decomposition, complete ensemble empirical mode decomposition with adaptive noise and artificial neural networks. Energy Convers Manage 2018;155:188–200.
[29] Huang G, Huang GB, Song S, et al. Trends in extreme learning machines: a review. Neural Networks, 2015, 61(C):32–48.
[30] Liu Hui, Mi Xiwei, Li Yanfei. Smart multi-step deep learning model for wind speed forecasting based on variational mode decomposition, singular spectrum analysis, LSTM network and ELM. Energy Convers Manage 2018;159:54–64.
[31] Zhang C, Zhou J, Li C, et al. A compound structure of ELM based on feature selection and parameter optimization using hybrid backtracking search algorithm for wind speed forecasting. Energy Convers Manage 2017;143:360–76.
[32] Wei S, Liu M. Wind speed forecasting using FEEMD echo state networks with RELM in Hebei, China. Energy Convers Manage 2016;114:197–208.
[33] Zheng W, Peng X, Lu D, et al. Composite quantile regression extreme learning machine with feature selection for short-term wind speed forecasting: a new approach. Energy Convers Manage 2017;151:737–52.
[34] Wang MD, Qiu QR, Cui BW. Short-term wind speed forecasting combined time series method and arch model. In: International Conference on Machine Learning and Cybernetics. IEEE, 2012. p. 924–27.
[35] Mi XW, Liu H, Li YF. Wind speed forecasting method using wavelet, extreme learning machine and outlier correction algorithm. Energy Convers Manage 2017;151:709–22.
[36] Liu H, Duan Z, Li YF. Big multi-step wind speed forecasting model based on secondary decomposition, ensemble method and error correction algorithm[J]. Energy Convers Manage 2018;156:525–41.
[37] Gilles J. Empirical wavelet transform. IEEE Trans Signal Process 2013;61(16):3999–4010.
[38] Huang GB, Zhou H, Ding X, et al. Extreme learning machine for regression and multiclass classification. IEEE Trans Syst Man & Cybernetics Part B, 2012, 42(2):513–29.
[39] Huang GB, Chen L, Siew CK. Universal approximation using incremental constructive feedforward networks with random hidden nodes[J]. IEEE Trans Neural Networks 2006;17(4):879–92.
[40] Mirjalili S, Mirjalili SM, Lewis A. Grey wolf optimizer. Adv Eng Softw 2014;69(3):46–61.